

JAERI - M
84-244

PALLAS-2DCY-FX : A CODE FOR DIRECT
INTEGRATION OF TRANSPORT EQUATION
IN TWO-DIMENSIONAL (R,Z) GEOMETRY

February 1985

Kiyoshi TAKEUCHI*, Nobuo SASAMOTO
and Yasuji KANAI**

日本原子力研究所
Japan Atomic Energy Research Institute

JAERI-Mレポートは、日本原子力研究所が不定期に公刊している研究報告書です。
入手の問い合わせは、日本原子力研究所技術情報部情報資料課（〒319-11茨城県那珂郡東海村）あて、お申しこしてください。なお、このほかに財団法人原子力弘済会資料センター（〒319-11茨城県那珂郡東海村日本原子力研究所内）で複写による実費頒布をおこなっております。

JAERI-M reports are issued irregularly.

Inquiries about availability of the reports should be addressed to Information Division
Department of Technical Information, Japan Atomic Energy Research Institute, Tokai-
mura, Naka-gun, Ibaraki-ken 319-11, Japan.

©Japan Atomic Energy Research Institute, 1985

編集兼発行 日本原子力研究所
印刷 榎高野高速印刷

PALLAS-2DCY-FX : A Code for Direct Integration of Transport
Equation in Two-Dimensional (R,Z) Geometry

Kiyoshi TAKEUCHI*, Nobuo SASAMOTO and Yasuji KANAI**

Department of Reactor Engineering,
Tokai Research Establishment, JAERI

(Received December 27, 1984)¹

The PALLAS-2DCY-FX program is the revised version of the PALLAS-2DCY code, which was designed in 1973 and revised in 1980, based on a method of direct integration of the Boltzmann transport equation to describe the radiation transport in (r,z) two-dimensional geometry. It has been developed for shielding problems involving the transport of neutrons and photons. A special feature of the present code is inclusion of the routine for analytical calculation of uncollided flux for accurate calculation of duct and void streaming or skyshine. The document gives a full description of input and output data, as well as code implementation information and a description of several demonstration problems.

keywords : Revised PALLAS-2DCY-FX Code, Direct Integration
Method, Two-Dimensional (r,z) Geometry, Shielding
Problems, Neutron Transport, Photon Transport
Analytical Calculation, Uncollided Flux

*Cooperative Research Scientist; Ship Research Institute

**Ship Research Institute

PALLAS-2DCY-FX : 2次元 (R, Z) 形状における
輸送方程式の直接積分コード

日本原子力研究所東海研究所原子炉工学部

竹内 清*・笹本宣雄・金井康二**

(1984年12月27日受理)

2次元 (r, z) 形状における放射線輸送計算を目的として、1973年に開発され、1980年に改訂されたボルツマン輸送方程式の直接積分法コードPALLAS-2DCYを改良、整備して、PALLAS-2DCY-FXを新たに作成した。本コードは中性子およびガンマ線の遮蔽計算用に開発されたものである。その主な特徴は、非散乱線束を解析的に計算するルーチンを備え、ダクトやボイド中のストリーミング問題、スカイシャイン問題を正確に計算できる点にある。本報告はコードの入出力データの詳細な説明を与えるものであり、あわせてコード使用の際に必要な情報および種々のテスト問題の計算例について記述している。

*) 協力研究員：船舶技術研究所

***) 船舶技術研究所

Contents

1.	Program abstract	1
2.	Introduction	3
3.	Information for users	5
3.1	Input specification	5
3.2	Detailed data notes	30
3.3	External and internal data files	46
3.4	Program mnemonics and program variables	46
3.5	Sample problems	47
3.6	Other notes	51
4.	Angular mesh points and nuclear data used in PALLAS code ..	52
4.1	Angular mesh points	52
4.2	Nuclear data for PALLAS	52
	References	54

目 次

1. プログラムの概要	1
2. 序 言	3
3. コード利用者のための情報	5
3.1 入力データの作成法	5
3.2 入力データについての詳細な説明	30
3.3 データファイル使用法	46
3.4 プログラム変数の意味	46
3.5 例 題	47
3.6 その他の注意点	51
4. PALLASコードの角度分点と核データ	52
4.1 角度分点	52
4.2 PALLASの核データ	52
参考文献	54

1. PROGRAM ABSTRACT

1. Name of Program : PALLAS-2DCY-FX
2. Computer for which designed or operable : FACOM M-380
3. Nature of physical problem solved : PALLAS-2DCY-FX solves the steady state Boltzmann transport equation in two-dimensional (r,z) geometry. Application is restricted to neutron and photon transport in a fixed-source problem.
4. Method of solution : The method of direct integration of the transport equation is used, in which the equation is integrated along the flight path of particle in the direction of motion at each discrete ordinate direction. Anisotropic scattering is treated precisely using differential scattering cross sections. No iteration and convergence techniques are used for determination of flux. To improve the accuracy of duct and void streaming calculations or skyshine calculations, a special option has been added : The uncollided angular flux from a point source or any cylindrical surface sources is calculated analytically based on the point kernel integration.
5. Restriction : About 3350KB are required for the total core storage for (75×75) spatial and 28 fixed directional meshes.
6. Typical running time : About 0.0030 sec/spatial mesh/group is required as cpu time on FACOM M-380.
7. Usual features : Fixed dimensioning is used, so that at least 2000Kb core storage is required. Nuclear data for neutron

shielding calculation are read in from the PALLAS library tape. Linear attenuation coefficients and pair production coefficients for photon are also read in from another PALLAS library.

8. Machine requirements : Card input, printed output, and scratch data sets may be located on defined external storage device.
9. Language : FORTRAN IV
10. Material available : Input description, source deck for FORTRAN routines and sample problems.

2. Introduction

The PALLAS-2DCY- FX computer code solves the energy and angular dependent Boltzmann transport equation with general anisotropic scattering in cylindrical geometry. Principal applications are to neutron or gamma-ray transport problems in forward mode. The code is particularly designed and suited to the solution of duct-and void-streaming and skyshine problems as well as deep penetration radiation transport problems with external source.

The code has been designed based on a method of direct integration of the transport equation¹⁾²⁾, in which the equation is solved by integrating along a flight path of radiation in the direction of motion at each discrete-ordinate angle. The specific features of this method are that (1) the radiation flux ($n/cm^2 \cdot sec \cdot (sr) \cdot MeV$) is calculated at each energy mesh without using any conventional iterative techniques used widely in S_n method for obtaining group flux at each energy group, and (2) the scattering source is calculated directly using the differential scattering cross section for neutron or the Klein-Nishina formula for gamma ray³⁾. Thus a Legendre polynomial expansion approximation used widely in S_n method is not applied to the calculation of radiation scattering. As a result PALLAS-2DCY can provide always positive and physically meaningful angular and scalar fluxes. Besides, (3) no supplementary difference equations are required to obtain a solution to the flux, which makes users free from bothering about choice of such modes as

"diamond difference", "step function" and "weighted difference" equations. By virtue of no usage of average flux, PALLAS-2DCY can be applied to even such problems as violently varied angular and spatial distributions of radiation flux⁴⁾. In contrast, Two-dimensional Sn codes calculate the transport equation based on the average flux for a cell with each pair of associated cell face fluxes in the five-dimensional finite cells defined in terms of location, direction, and energy phase space variables.

The weak point in the present PALLAS-2DCY-FX code is that it has been written in the fixed dimensioning, which restricts the numbers of energy meshes (≤ 100 for neutron and for photon), material regions (10×10), nuclides (≤ 25), angular meshes (28), spatial meshes (75×75) to be inputed.

The neutron cross sections required by PALLAS-2DCY are taken from the PALLAS library. On the other hand the gamma-ray cross sections are also taken from another PALLAS gamma library.

An analytic uncollided flux calculation option is available in the PALLAS-2DCY-FX code for a variety of source geometries such as a point, line, disk and cylindrical volume sources. The original PALLAS-2DCY code was written for CDC6600 computer in 1973⁵⁾ to calculate neutron transport in shields. Revisions have been made to the old version so as to calculate neutron and gamma ray transport in shields⁶⁾ and also to deal with not only a cylindrical volume source but also various boundary source problems including a point source.⁷⁾

3. INFORMATION FOR USERS

3.1 Input Specification

Card 1 Title card PROBLEM (20A4)

Card 2 Control Integers for a PROBLEM

KNDG, KIN, NORF, KTST, MONOE, MNODRE, IPRNT, IRZZR, IRTZ (9I3)

KNDG=1, neutron calculation.

=2, neutron-secondary gamma-ray calculation.

=4, photon calculation.

KIN=0, no effect.

=n, n coupled neutron calculations (data note 1).

NORF=0, reflection boundary condition at the bottom boundary.

>0, no reflection at the bottom or Z-axis boundary.

KTST=0, no effect.

=-1, check of input data read in and no transport calculation.

=103, test calculation up to 103-the energy mesh.

MONOE=0, no effect.

=2, monoenergy source+continuous energy source (data note 2).

=10, monoenergy problem (data note 2).

MNODRE=0, gamma-ray isotropic incidence (data note 3)

=1, gamma-ray normal incidence (data note 3)

=n, gamma-ray slant incidence (data note 3)

IPRNT=0, no effect.

>0, Legendre coefficient FMU and inelastic scattering slowing down matrix CIB are printed for neutron

nuclear data. Library data are printed for gamma-ray nuclear data.

Calculated scalar fluxes within the monoenergy neutron group are printed for monoenergy calculation.

IRZZR=0, no effect.

>0, conversion of calculated angular flux in (R,Z) coordinate into those in (Z,R) coordinate.

IRTZ=0, no effect.

≠0, conversion of calculated angular flux in (R,Z) coordinate into those in (R,θ,Z) coordinate.

<0, read NITP21 (total energy mesh).

Repeat n times from card 3 if KIN=n>0.

Card 3 JJ, IR, IZ, IUNCL, IFIS, NNI, JSAT, IQIQ (8I3)

JJ=number of energy meshes ≤ 100 for neutron and for photon.

IR=number of r-regions ≤ 10 .

IZ=number of z-regions ≤ 10 .

IUNCL=0, no effect.

=n, unscattered angular fluxes are calculated up to n-th energy mesh by the analytical calculation based on the point kernel integration.

=-n, unscattered angular fluxes are calculated up to n-th energy mesh after the transport calculation at each energy mesh (data note 4)

IFIS=0, source energy spectrum S(E) is read in from cards.

=1, fission spectrum is defined in the program. Do not enter S(E). The fission spectrum is calculated in the

program: $S(E) = 0.484 \sinh\sqrt{2E} \cdot e^{-E}$ for neutron,
 $= 14.0 \exp(-1.10E)/12.7$ for photon.

NNI=0, nuclear library for neutron is set at File unit 1.

=n>50, nuclear library for neutron is set at File unit n.

Note: Nuclear data for photon are always read in from
 File unit 31.

JSAT=0, no effect.

=n, neutron transport calculation starts at n-th ($n > 1$)
 energy mesh. Flux calculation up to (n-1)-th energy
 mesh is omitted.

IQIQ=0, no effect.

>0, polar angular meshes (WP(ip), ip=1, 8) are read in
 from cards.

Weights for WP(ip) are read in from cards.

Boundaries WBP(ip) are read in from cards.

Weights for angular meshes (WPQ(ipQ), ipQ=1, 28) are
 read in from cards.

Card 4 NBND, IBZ1, IBZ2, IBR, LTAP, JOAK, IRWTR (7I3)

NBND=0, cylindrical volume source problem.

=1, point source (data note 5).

=10, boundary flux problem.

IBZ1=z mesh at which top boundary is defined (data note 6).

IBZ2=z mesh at which bottom boundary is defined (data note
 6).

IBR=r mesh at which cylindrical surface boundary is defined
 (data note 6).

LTAP=0, no effect.

=22, boundary fluxes are read in from Tape 22 in which angular fluxes calculated previously have been stored.

=25, boundary fluxes are read in from Tape 25 and used for the present transport calculation without interpolations (data note 7).

JOAK=0, no effect.

=n, print boundary angular fluxes up to n-th energy mesh for check.

IRWTR=0, no effect.

=1, weight function for heavy materials.

=2, weight function for sodium deep penetraton.
(data note 8).

Card 5 EMAX, HH, SNORM, RDST (4E10.3)

EMAX=maximum energy in MeV.

HH=energy mesh interval for gamma ray calculation, and if

HH=0.0, all the energy meshes are read in from Card 10.

=lethargy interval for neutron (0.05, 0.1, 0.2 or 0.4).

SNORM=source normalization for source volume,

$$\iint S(r,z) dr dz = \text{SNORM}.$$

RDST=0, no effect.

>0, first radial distance in cm, which is used in the case of NBND=1.

Card 6 MER(n), n=1, IR (10I3)

Number of meshes in n-th radial region.

Card 7 RR(n), n=1, IR (8E10.3)

Thickness in cm in n-th radial region (data note 9).

Card 8 MEZ(n), n=1, IZ (10I3)

Number of meshes in n-th axial region.

Card 9 ZZ(n), n=1, IZ (8E10.3)

Thickness in cm in n-th axial region.

Card 10 E(j), j=1, JJ (8E10.3)

Photon energy at j-th energy mesh in MeV if HH=0.0. Do not enter them for neutron because neutron energies are defined by an equal lethargy interval:

$$E(j) = E_{MAX} \times \exp(-(j-1) \times HH).$$

When IQIQ>0 in Card 3, the following four cards are inputed.

Card 10-A WP(ip), ip=1,8 (8E10.3)

Polar angular meshes (cosin θ ip).

Card 10-B WWP(ip), ip=1,8 (8E10.3)

Weights for WP(ip)'s.

Card 10-C WBP(ip), ip=1,8 (8E10.3)

Boundaries for WP(ip)'s.

Card 10-D WPQ(ipq), ipq=1,28 (8E10.3)

Weights for Ω_{pq} .

There are five options for Card 11 in accordance with several source problems: Type A is a cylindrical volume source indicated by NBND=0, type B is a point source problem indicated by NBND=1, type C is a top or bottom boundary problem indicated by NBND=10, LTAP=0, IBZ1>0 or IBZ2>1, in which LTAP=0 means that the boundary flux is read in from cards. Type D is also a top or

bottom boundary problem indicated by NBND=10, LTAP=22 or 25, IBZ1>0 or IBZ2>1, in which LTAP=22 or 25 means that the boundary flux is taken from the data stored in File unit 22 or 25. Type E is cylindrical surface boundary problem indicated by NBND=10, LTAP, IBR>0.

Type A: NBND=0, the volume source is expressed by

$$S(r,z,E)=S(r)\times S(z)\times S(E) \text{ n/cm}^3\cdot\text{sec}\cdot\text{MeV (Type 1)},$$

or

$$S(r,z,E)=S(r,z)\times S(E) \text{ n/cm}^3\cdot\text{sec}\cdot\text{MeV (Type 2)}.$$

Card 11-A-1 MSR, MSZ, IVS (3I3)

MSR=r-mesh number up to which radial source distribution is read in:

$$S(r_n) \quad n=1, \dots, \text{MSR}.$$

MSZ=z-mesh number up to which axial source distribution is read in:

$$S(z_n) \quad n=1, \dots, \text{MSZ}.$$

IVS=0, Type 1.

>0, Type 2.

Card 11-A-2 SRMIN, SRMAX, SZMIN, SZMAX (4E10.3)

SRMIN, SRMAX=a volume source is defined between SRMIN and SRMAX in radius in cm.

SZMAX=top axial distance of cylindrical source in cm.

SZMIN=bottom axial distance of cylindrical source in cm.

(data note 10).

Card 11-A-3 SR(n), n=1, MSR (8E10.3)

If IVS=0, $S(r_n)$, $n=1, \dots$, MSR.

Card 11-A-4 SZ(n), $n=1, \dots$, MSZ (8E10.3)

If IVS=0, $S(z_n)$, $n=1, \dots$, MSZ.

Card 11-A-3 SRZ(m,n), $m=1, \dots$, MSR), $n=1, \dots$, MSZ) (8E10.3)

If IVS>0, source spatial distribution $S(r,z)$ are defined.

Card 11-A-5 SE(j), $j=1, \dots$, JX** (8E10.3)

Source energy spectrum (/MeV) if IFIS=0. Do not enter if IFIS>0. **JX=JJ for MONOE=0 or 1 for MONOE=10.

Type B: NBND=1, a point source option.

Card 11-B-1 LIAG, JIAG (2I3)

LIAG=0, isotropic source and >0, anisotropic source.

JIAG=0, MONOE=10 and JIAG>0, MONOE=0.

Card 11-B-2 SE(j), $J=1, \dots$, JX** (8E10.3)

Source spectrum (/MeV) if IFIS=0. Do not enter if IFIS>0.

Card 11-B-3 B(J1,Ip), $Ip=1, 28/J1=1, \dots$, JIAG (8E10.3)

Angular distribution of an anisotropic source if LIAG>0.

Type C: NBND=10, LTAP=0, IBR=0, IBZ1>0, IBZ2>1, the top or bottom boundary flux is expressed by

$$\text{BOUN}(\bar{\Omega}, r) = S(r, \bar{\Omega}) \cdot S(E) \text{ n/cm}^2 \cdot \text{sr} \cdot \text{sec} \cdot \text{MeV at } E,$$

for $\bar{\Omega} > 0$ with respect to Z axis, or

$$\text{BNMZ}(\bar{\Omega}, r) = S(r, \bar{\Omega}) \cdot S(E) \text{ n/cm}^2 \cdot \text{sr} \cdot \text{sec} \cdot \text{MeV at } E,$$

for $\bar{\Omega} < 0$ with respect to Z axis.

Card 11-C-1 LRMIN, LRMAX, ISOC, ICONT, IRPT, IXR, IYR (7I3)

LRMIN, LRMAX=r-mesh number within which boundary fluxes

are read in from cards.

ISOC=0, angular distribution of boundary flux is read in from cards.

=1, isotropic angular distribution is defined in the program.

ICONT=0, radial distribution of boundary flux is read in from cards.

=1, constant radial distribution is assigned in the program.

IRPT=0, boundary distributions are read in at each energy mesh, $j=1, JX^{**}$.

IRPT>0, boundary distributions are same ones for all the energy meshes. The data are read only for $j=1$.

IXR and IYR; print the boundary fluxes at r meshes from IXR through IYR meshes for check.

Card 11-C-2 SE(j), $j=1, JX^{**}$ (8E10.3)

Source energy spectrum (/MeV) if IFIS=0. Do not enter if IFIS>0.

Card 11-C-3-1 SN(m,ip), $ip=ip1, ip2/m=LRMIN, LRMAX$ (8E10.3)

Angular fluxes at each r mesh ($LRMIN \leq r < LRMAX$) in units of $n/cm^2 \cdot sr \cdot sec \cdot MeV$ if ISOC=ICONT=0.

$ip1=1$ and $ip2=14$ for IBZ1>0.

$ip1=15$ and $ip2=28$ for IBZ2>0.

Card 11-C-3-2 SN(ip), $ip=ip1, ip2$ (8E10.3)

Angular fluxes with constant radial distribution if ISOC=0 and ICONT=1.

Card 11-C-3-3 SN(m), m=LRMIN, LRMAX (8E10.3)

Radial distribution with isotropic angular distribution if
ISOC=1 and ICONT=0.

Note if ISOC=1 and ICONT=1 do not enter Card 11-C-3.

Type D: NBND=10, LTAP=22, IBR* , IBZ1>0 or IBZ2>1, the top or
bottom boundary flux is taken from the data stored in
File Unit 22. *IBR = 0 or \neq 0.

Card 11-D-1 LRR, LZZ, LZZ1, LZZ2, LRMIN, LRMAX, IXR, IYR (8I3)

LRR=total number of r meshes in an old calculation stored
in File unit 22.

LZZ=total number of z meshes in an old calculation.

LZZ1=z-mesh number in LZZ meshes at which calculated
angular fluxes are picked up for the top boundary
fluxes in a new calculation (data note 11).

LZZ2=z-mesh number in LZZ meshes at which calculated fluxes
are picked up for the bottom boundary fluxes in a new
calculation (data note 11)

LRMIN, LRMAX= r-mesh numbers between which the boundary
fluxes are defined for a new calculation.

IXR and IYR are the same as defined before.

Card 11-D-2 ROLD(i), i=1, LRR (8E10.3)

R distances in cm at R meshes used in an old calculation
(LTAP=22).

If LTAP=25, ROLD(i) are ignored.

Type E: NBND=10 and IBR>0, cylindrical surface fluxes are defined at IBR-th radial mesh.

Card 11-E-1 LZMIN, LZMAX, IRPT, IXZ, IYZ (5I3)

Boundary fluxes are set at z meshes from LZMIN-th through LZMAX-th mesh (data note 12)

IRPT=0 or >0.

IXZ and IYZ; boundary fluxes are printed at z meshes from IXZ through IYZ-mesh for check.

For LTAP=0,

Card 11-E-2 BOUNR(ip,m), ip=1, IQT/m=LZMIN, LZMAX (8E10.3)

Angular distribution at each z mesh in units of $n/cm^2 \cdot sr \cdot sec \cdot MeV$. Repeat from the first through last energy mesh if IRPT=0.

For LTAP=22 or 25,

Card 11-E-2' LRR, LZZ, LRRL (3I3)

LRR=total number of r meshes in an old calculation.

LZZ=total number of z meshes in an old calculation.

LRRL=r-mesh number in LRR meshes at which calculated

angular fluxes are picked up for the surface boundary fluxes in a new calculation (data note 12).

Card 11-E-3' ZOLD(n), n=1 LZZ (20I3)

z distances in cm at z meshes in an old calculation (LTAP=22).

If LTAP=25, ZOLD(n) are ignored.

Note if IBR = 0, do not enter Card 11-E.

Card 12 LTHAL, LCUT (2I3)

LTHAL=0, no effect.

>0, execute thermal group calculation (data note 13).

LCUT=0, no effect.

=n, termination of iterative thermal group calculations.

Note if $KNDG > 3$ do not enter this card.

Card 13 EPSRN (E10.3)

Convergence criterion. Do not enter this card if $KNDG > 3$.

Card 14 NOEL(i,j), j=1, IR/i=1, IZ (10I3)

Number of nuclides in each material region (data note 14).

Maximum number of nuclides in all the regions of a problem = 25 (fixed).

Card 15 NEK(i,j), j=1 IR/i=1, IZ (10I3)

Number of material identification (data note 15).

If IUNCL≠0, Cards 16 and 17 are required.

Card 16 KSR1, KBR1, KZT1, KBZ1, KZB1, KBBZ1, NPFI (7I3)

Radial mesh specification for source (from 1 to KSR1-th mesh) and axial mesh specification for source (from KZB1-th to KZT1-th mesh). Material region number in radial direction for KSR1-mesh is KBR1. Material region numbers in axial direction for KZT1 and KZB1 are KBZ1 and KBBZ1, respectively (data note 16).

NPFI=0, NPFI=4 is set.

=n, n=6 or 8 (data note 16).

Card 17 IUNC(i,j), j=1, IR/i=1, IZ (10I3)

Unscattered angular flux calculation is made in the spatial regions defined by IUNC(i,j)=1 in addition to scattered angular flux calculation.

If IUNCL<0, Card 18 and 19 are required.

Card 18 KSR2, KBR2, KZT2, KBZ2, KZB2, KBBZ2 (6I3)

Card 19 IUNB(i,j), j=1, IR/i=1, IZ (10I3)

Only unscattered angular flux calculation is made in the region specified by IUNB(i,j)=1 (data note 17).

If IRWTR≠0, the following Card 19-A is required for specifying the material regions in which the weight functions are applied (data note 8).

Card 19-A IWTR(i,j), j=1, IR/i=1, IZ (10I3)

The input data described below are for nuclear data read in repeatedly every material.

Card 20 MATERIAL (6A4)

Name of material.

For neutron data (KNDG \leq 2),

Card 21 NUCLID, INPTP (2A4, I5)

NUCLID=symbol of nuclide.

INPTP=0, nuclear data are read in from PALLAS library.

>0, nuclear data are read in from cards.

In the case of INPTP=0,

Card 22 MATNO, AN(NUC), AMAS, ICH (I5, 2E10.3, I3)

MATNO=material number (4 digits given in Table 2).

AN(NUC)=nuclear density ($\times 10^{24}$).

AMAS =mass of nuclide.

ICH=0, no effect.

>0, $\sigma_t(E_j)$ and $\sigma_{el}(E_j)$ are read in from cards, by which

the data on total and elastic scattering cross sections

read in from the library are replaced (data note 18).

In the case of ICH>0,

Card 23 LCH(n), n=1, ICH

Energy meshes at which the data are replaced.

If ICH=JJ, this card is ignored because all the energy meshes are used.

Card 24 SIGT(j), j=LCH(1), LCH(ICH) (8E10.3)

$\sigma_t(E_j)$, microscopic total cross section at energy E_j (barn).

Card 25 SIGMA(j), j=LCH(1), LCH(ICH) (8E10.3)

$\sigma_{el}(E_j)$, microscopic elastic scattering cross section at E_j (barn).

In the case of INPTP>0,

Card 21 AMAS, AN(NUC) (2E10.3)

Card 22 SIGT(j), j=1, JJ (8E10.3)

Card 23 SIGMA(j), j=1, JJ (8E10.3)

Card 24 LL, JLL (2I3)

LL=order of Legendre polynomial expansion.

JLL=energy-mesh number up to which Legendre expansion coefficients are read in.

Card 25 FMU(j,l), l=1, LL/j=1, JLL (8E10.3)

Legendre expansion coefficients; $f_l(E_j)$ (data note 19).

Card 26 INEL (I3)

INEL=0, neither inelastic scattering nor (n,2n) data are read in.

INEL>0, inelastic scattering and/or (n,2n) data are read in

For INEL>0,

Card 27 JIN, J2N (2I3)

JIN=0, no inelastic scattering data.

JIN=n, inelastic scattering data are read in from cards up to n-th energy mesh;

$\sigma_{in}(E_k, E_j)$, k=1, ---, n/j=1, ---JJ.

J2N=0, no (n,2n) data.

J2N=n, (n,2n) data are read in from cards up to n-th energy

mesh;

$$\sigma_{n,2n}(E_k, E_j), k=1, \dots, n/j=1, \dots, JJ.$$

card 28 SN(k,j), k=1, J2N/J=1, JJ (8E10.3)

Slowing down cross section from E_k to E_j energy per MeV due to (n,2n) reaction. Isotropic scattering in the laboratory system is assumed. If J2N=0, do not enter them (data note 20).

Card 29 CIB(k,j), k=1, JIN/j=1, JJ (8E10.3)

Slowing down cross section from E_k to E_j per MeV due to inelastic scattering. Isotropic scattering in the laboratory system is assumed. If JIN=0, do not enter them.

For photon data (KNDG=4).

For NOEL (N1, N2)>0, nuclear data are read in from PALLAS library set at File unit 31.

Card 21 MATN(N), N=1, NOEL(N1, N2) (10I3)

MATN(N)=material number (3 digits in 4 digits given in Table 2, i.e., 260 for Fe which corresponds to 1260 in Table 2)

Card 22 BNUC(N), BNE(N), DENSI (3E10.3)

N=1, NOEL(N1, N2)

BNUC(N)=nuclear density ($\times 10^{24}$).

BNE(N)=binding energy in MeV.

DENSI=material density (g/cm^3) if NOEL(N1, N2)=1, and if NOEL(N1, N2)>1, DENSI=0.0.

For NOEL(N1, N2)=0, no data are read in.

For NOEL(N1, N2)<0, nuclear data are read in from cards.

Card 21 EDN(N1, N2) (E10.3)

Electron density ($\times 10^{24}$) in (N1, N2)-th material region.

Card 22 CRT(N1, N2, j), J=1, JJ (8E10.3)

Linear attenuation coefficient (cm^{-1}) at gamma-ray energy

E_j in (N1, N2)-th material region (data note 21).

Card 23 SIGMA(j), j=1, JJ (8E10.3)

Linear pair production coefficient (cm^{-1}) at gamma-ray

energy E_j in (N1, N2)-th material region.

Input data specifying external data and output.

Card-01 ITP20, ITP21, KANK, ISKIP, ITP24, ITP29 (6I3)

ITP20=0, no effect.

=J, calculation starts using the old calculated data stored in File unit 20.

ITP21=0, no effect.

>0, calculated angular fluxes are stored in File unit 21.

=5, input data used in a calculation are also stored in File unit 21 for use in plotting energy spectrum, attenuation and dose map.

=10, limited number of calculated angular fluxes are stored in File unit 21.

For the limitation, Card-02 is prepared.

KANK=0, no effect.

=1, or 2, if ITP20>0 (data note 22)

ISKIP=0, no effect.

=k, skip k groups from the first group when reading the old data from File unit 20.

ITP24=0, no effect.

=1, calculated reaction rates (or dose rates) are stored in File unit 24.

ITP29=0, no effect.

=1, calculated scalar fluxes are stored in File unit 29.

Card-02 LR1, LR2, LZ1, LZ2 (4I3)

Calculated angular fluxes at radial meshes between LR1 and LR2 and at axial meshes between LZ1 and LZ2 are stored at File unit 21 if ITP21=10. If ITP21≠10, no data are prepared.

Card-03 MRK, MZK, MDS, MZDS, IEF, NOR1, NOR2, NOZ1, NOZ2 (9I3)

MRK=0, no angular fluxes are printed.

>0, number of r meshes at which angular fluxes are printed.

MZK=0, no angular fluxes are printed.

>0, number of z meshes at which angular fluxes are printed.

MDS=0, only dose rate (in units of mrem/h) are printed.

=n, n reaction rates are printed (maximum number is 14).

MZDS=0, no effect.

>0, currents at MZDS-th z mesh for +z direction and -z direction are printed at all radial meshes.

IEF=0, angular and scalar fluxes are printed in units of $n/cm^2 \cdot sec(sr)MeV$.

=1, energy angular and scalar fluxes are printed in units of $MeV/cm^2 \cdot sec(sr)MeV$.

NOR1=NOR2=NOZ1=NOZ2=0, all the calculated scalar fluxes are printed.

NOR1>0, NOR2>0, NOZ1>0, NOZ2>0, scalar fluxes are printed at r meshes from NOR1-th through NOR2-th and at z meshes from NOZ1-th through NOZ2-th (data note 23).

Card-04 KR(n), n=1, MRK (20I3)

Radial mesh numbers at which angular fluxes are printed if
MRK and MZK >0 (data note 24).

Card-05 KZ(n), n=1 MZK (20I3)

Axial mesh numbers at which angular fluxes are printed if
MRK and MZK >0 (data note 24).

Card-06 REACT (20A4)

Name of reaction in n-th reaction (or dose rate, for
instance mrem/h).

Card-07 DOSE(j,n), j=1, JJ (8E10.3)

Reaction cross section (or dose rate conversion factor) at
energy E_j in n-th reaction.

Input data for conversion of calculated angular fluxes in (r,z) geometry to those in (z,r) geometry.

This conversion is used for a new transport calculation in (\bar{r},\bar{z}) geometry based on already calculated angular flux in (r,z) geometry. Here the (\bar{r},\bar{z}) geometry corresponds to 90-deg conversion of the original (r,z) geometry (data note 25).

Card-RZ-1 MRRL, MZCNTR, KDR, NWRB, LRL, IPR, MZ1, MZ2, NF, HH
(9I3, F12.4)

MRRL=r-mesh number at which angular fluxes are picked up.

MZCNTR=origin of new (r,z) geometry.

KDR=0; boundary fluxes are taken from MZCNTR to +z direction in old (r,z) geometry.

=-1; boundary fluxes are taken from MZCNTR to -z direction in old (r,z) geometry.

NWRB=new boundary fluxes in new (\bar{r},\bar{z}) geometry are specified between NWRB-th r mesh and LRL-th r mesh.

IPR=0; no list.

≠0; currents in old and new geometries and their ratio as well as old angular fluxes between MZ1 and MZ2 are printed.

NF=0; no effect.

≠0; normalization factor.

HH=0.0; no effect.

=lethargy width for neutron monoenergy source.

Card-RZ-2 ANF (E10.3)

Normalization factor if $NF \neq 0$.

This card is neglected if $NF=0$.

Card-RZ-3 RN(MR),MR=1, LRL (8E10.3)

Radial distance at MR-th mesh in new (\bar{r}, \bar{z}) geometry when its center corresponds to MZCNTR.

Note that the old and new boundary angular fluxes are stored in Files 21 and 35, respectively.

Input data for preparing boundary angular fluxes in (r, θ, z) geometry for three-dimensional PALLAS-RTZ code.

The boundary angular fluxes for PALLAS-RTZ code are made by converting the angular fluxes at r_i meshes ($i=1, 2, \dots, LR2$) at $z=LZ1$ mesh calculated in (r, z) geometry to those at radial meshes in (r, θ, z) geometry. Figure 13 illustrates an example of the conversion, where \bar{z} axis is always taken to be parallel to z axis.

Card-T-1 RZRO (E10.3)

The position of a new \bar{z} axis in $(\bar{r}, \bar{\theta}, \bar{z})$ geometry, which is measured from the origin of (r, z) geometry.

Card-T-2 IRMS, ITMS (2I3)

IRMS=total number of radial meshes defined in (r, θ, z) geometry.

ITMS=total number of azimuthal (θ) meshes in (r, θ, z) geometry.

Card-T-3 RTZ(i), i=1, IRMS (8E10.3)

Radial distances at i meshes in (r, θ, z) geometry.

Card-T-4 TRZ(i), i=1, ITMS (8E10.3)

Azimuthal angle (in radian) at i -th θ mesh ($0 \leq \theta_i \leq 3.1416$).

Card-T-5 PRTZ(i, j), j=1, 8/i=1, 4 (8E10.3)

Azimuthal angle of radiation moving direction (in radian) in (r, θ, z) geometry.

Card-T-6 WPQ3(ip), ip=1, 24 (8E10.3)

Weights for Ω_{pq} of radiation moving direction in (r, θ, z)

geometry.

Card-T-7 IRPR (I3)

IRPR=0, no check print.

≠0, check print.

When one wants to use this conversion, one should specify as IRTZ≠0 in Card 2 and also specify as ITP21=10 in Card-O1 and LR1=1, LR2>LR1, LZ1=LZ2>0 in Card-O2. Then, the calculated angular fluxes in (r,z) geometry are picked up between LR1- and LR2- radial mesh at LZ1-th z mesh at each energy mesh to store in File unit 21.

In the case shown in Fig.13 the new boundary angular flux is defined for $+\bar{r}$ direction, however it can be defined also for $-\bar{r}$ direction from the new origin in (\bar{r},θ,\bar{z}) geometry, since the radial distances in (\bar{r},θ,\bar{z}) geometry are measured from the new origin.

The new boundary angular fluxes at each energy mesh are stored in File unit 25.

Input data for secondary gamma-ray transport calculation when KNDG=2.

Card-S-1 JJ, IR, IZ, IUNCL, IFIS (5I3)

JJ=25, (fixed for secondary gamma-ray calculation; see Table 4).

IR and IZ are same as in Card 3.

IUNCL may be defined newly for a gamma-ray calculation.

IFIS is specified for a primary gamma-ray calculation.

Card-S-2 NBND, IBZ1, IBZ2, IBR, LTAP, JOAK (6I3)

These input data are prepared for a primary gamma-ray transport calculation.

For no primary calculation, a blank card is prepared.

Card-S-3 EMAX, HH, SNORM, RDST (4E10.3)

EMAX=13.0 (maximum energy of secondary gamma rays, see Table 4).

HH=0.0.

SNORM=source normalization for primary gamma-ray source volume.

RDST is same as in Card 5.

Card-S-4=Card 11

This card is the same card as Card 11.

The input data for Card-S-4 are prepared according to specification of NBND for a primary gamma-ray transport calculation.

If IUNCL \neq 0, the following four cards must be prepared, however for IUNCL=0, no preparation is necessary.

Card-S-5 KSR1, KBR1, KZT1, KBZ1, KZB1, KBBZ1, NPHI (7I3)

The meaning of these input data is same as that of Card 16.

Card-S-6 IUNC(i,j),J=1, IR/i=1,iz (10I3)

Card-S-7 KSR2, KBR2, KZT2, KBZ2, KZB2, KBBZ2 (6I3)

Card-S-8 IUNB(i,j),j=1, IR/i=1,iz (10I3)

After inputting these S cards, additional input data specifying external data and output, Card-01 ~ Card-07, must be prepared for the output list of the gamma-ray transport calculation.

3.2 Detailed data notes

(1) Data note 1

The PALLAS neutron transport calculations are usually made based on the nuclear data from the PALLAS library, in which the energy mesh structures are defined depending upon the lethargy width as shown in Table 1. The structure of 0.1 lethargy width is recommended for fast neutron transport calculation and the structure of 0.2 lethargy width is recommended for the intermediate energy range. The structure of 0.4 lethargy width may be used for calculation in the low energy range including thermal group. The other combinations of structures can be utilized, for instance the 0.2+0.4+0.8 lethargy-width structure or the 0.2+0.4 lethargy-width structure. It should be desirable from the viewpoint of accuracy of calculated result to use the combination of 0.1+0.2+0.4 lethargy-width structure.

For reference, an example of the accuracy of the series calculations is given in the following: The problem is a neutron transport in a water+iron configuration for the fission source from a reactor core as shown in Fig.1. The transport calculations were made with three energy-mesh structures — composed of 27-energy(0.1 lethargy)+35-energy(0.2 lethargy)+45-energy(0.4 lethargy) meshes, of 35-energy(0.2 lethargy)+45-energy(0.4 lethargy) meshes, and of 25-energy(0.2 lethargy)+29-energy(0.4 lethargy)+23-energy(0.8 lethargy) meshes as shown in Fig.2.

The calculational accuracy of these transport calculations is provided as the ratios of B-structure/A-structure and of C-

structure/A-structure in Fig.3. The ratios are taken for three reactions — neutron fluence (>0.1 MeV), $In(n,n')$ reaction rate and dose rate. For all the reactions the structures starting with 0.2-lethargy interval provide 20 ~ 30 % underestimated values. From this fact it should be essential to use the structure of 0.1-lethargy interval in the higher energy region (at least MeV region).

When one uses the series calculation of lethargy-width structures, one should input an integer of 1 or 2 into the KIN; in the case of KIN=2, the structure composed of 0.1+0.2+0.4 or 0.2+0.4+0.8 lethargy widths can be used, while in the case of KIN=1, the structure composed of 0.1+0.2 or 0.2+0.4 lethargy widths can be used. If KIN=0, only one structure is used. As seen in Fig.2 for KIN >0 , the calculated angular fluxes at energy meshes of odd numbers are picked up for use in the next series calculation.

(2) Data note 2

Since the PALLAS calculation is made based on the continuous source energy distribution for the purpose of avoiding iterative calculation, it is inevitable to use a special treatment for calculation of mono-energy source problems. Thus in the case of a mono-energy source problem one should input as MONOE=10.

When a source energy spectrum is composed of a high intensity mono-energy source and a low intensity continuous energy source, one should specify as MONOE=2. In this case the

special treatment of the first energy mesh as MONOE=10 and the ordinary treatment of the other energy meshes as MONOE=0 are made in the program.

(3) Data note 3

The input MNODRE is used for calculations of gamma-ray isotropic or perpendicular or slant incidence on slab shields. In the case of MNODRE=2,3 and 4, the incident angles are respectively 24.3° , 50.3° and 77.3° .

(4) Data note 4

When one wants to calculate radiation flux in space behind shields as shown in Fig.4, one may input IUNCL=-n. Then the radiation flux within the shields is calculated using the analytical unscattered flux calculation technique at each energy mesh. After that the radiation flux leaking out from the outermost shield is calculated again using the analytical unscattered flux calculation technique based on the newly defined assumed source region as illustrated in the figure. This operation is repeated up to n-th energy mesh.

(5) Data note 5

A point source is defined at a certain position $Z=Z_0$ on the z axis.

(6) Data note 6

The top, bottom and cylindrical surface boundary conditions are defined as illustrated in Fig.5. In the case of only a top boundary problem, one may input $MZZ > IBZ1 > 0$ and $IBZ2 = IBR = 0$. In the case of only a bottom boundary problem, one may input $MZZ > IBZ2 > 0$ and $IBZ1 = IBR = 0$. In the case of a cylindrical surface problem, one may input $MRR > IBR > 0$ and $IBZ1 = IBZ2 = 0$. In the case of a top-bottom-cylindrical surface problem, one may input $MZZ > IBZ1 > IBZ2 > 0$ and $MRR > IBR > 0$. Here MRR and MZZ are respectively the maximum numbers of r and z spatial meshes.

(7) Data note 7

For a bootstrap type calculation, the first radiation transport calculations are stored in Tape 21 as described later. Then the second calculation is made based on the data stored in Tape 22 (=Tape 21) by specifying as $LTAP=22$. While for $LTAP=25$, the data calculated previously using the PALLAS code or the other transport codes are converted to fit the boundary fluxes for a new transport calculation. Consequently, the new transport calculation can start using the boundary fluxes taken from Tape 25.

(8) Data note 8

The neutron spectrum becomes to show abrupt increase in the energy region between several MeV and several hundred KeV with increasing penetration distances in heavy materials such as iron.

PALLAS calculation with the 0.1 lethargy interval structure, however, underestimates the energy spectrum in this energy region at penetration distances beyond 30 cm in an iron shield. This is attributed to the use of rough lethargy interval compared with that of maximum neutron slowing down in a single elastic scattering. To overcome this difficulty a weight function is introduced to estimate the rising gradient of the spectrum in the energy region at each material region in which the use of the weight function is indicated as IWTR>0. Though this technique is useful as a first approximation, more rigorous treatment should be made as soon as possible.

(9) Data note 9

An equal spatial mesh interval is defined in each spatial region: n-th radial thickness divided by (MER(n)-1) intervals gives the equal radial mesh interval in n-th region except for first radial region in which its thickness is divided by MER(1) intervals because of no radial mesh assignment at r=0 cm. In PALLAS spatial mesh assignment, two meshes must be assigned at every inner boundary as illustrated in Fig.6.

(10) Data note 10

As depicted in Fig.7 the radius and positions of top and bottom of the cylindrical volume source are specified by input data.

(11) Data note 11

As shown in Fig.8 the angular fluxes calculated previously are picked up at all the radial meshes from first through LRR-th at LZZ1-th z mesh in an old calculation. These fluxes will be used for top boundary fluxes at IBZ1-th z mesh in a new calculation. Since the positions of radial meshes in a new calculation are not necessarily identical with those of an old calculation, the top boundary fluxes will be determined for radial meshes from LRMIN through LRMAX-th in a new calculation by a linear interpolation.

(12) Data note 12

For cylindrical surface boundary fluxes the angular fluxes calculated previously are picked up at all the axial meshes from first through LZZ-th at LRRL-th r mesh in an old calculation. These fluxes will be used for the surface boundary fluxes at axial meshes from LZMIN-th through LZMAX-th at IBR-th radial mesh as depicted in Fig.9. Since the positions of axial meshes are not necessarily identical in between an old and a new calculations, the surface boundary fluxes will be calculated for axial meshes from LZMIN-th through LZMAX-th in a new calculation by a log-linear interpolation.

(13) Data note 13

It is inevitable for the thermal neutron flux calculation to use the conventional group calculation using an iteration-

convergence technique. For only the case of neutron thermal flux calculation LTHAL has a value larger than zero.

The iterative calculations continue until the following convergence criterion is satisfied for all the spatial meshes defined in a problem:

$$\text{Max} \left\{ \frac{\phi^n(\bar{r}) - \phi^{n-1}(\bar{r})}{\phi^n(\bar{r})} \right\} < \text{EPSRN},$$

where $\phi^n(\bar{r})$ is the scalar flux in n-th iteration.

(14) Data note 14

One of characteristics in the method used in PALLAS code is to deal with as precisely as possible radiation scattering calculations. For this purpose PALLAS executes the scattering calculation for each nuclide. Then one must specify the number of nuclides in each material region. As an ideal way the number of all nuclides included in each material should be specified, which however is not realistic from the point of view of computation time. One of practical ways is to choose the number of main nuclides which contribute considerably to the value of total cross section in each material region. In this limitation the other unimportant nuclides should be assigned to the main nuclides regarding nuclear density.

For instance, atomic compositions of concrete are assumed to be that Si; $0.0141(\times 10^{24})$, Al; 0.00295, Fe; 0.000764, Ca; 0.00294, Mg; 0.000483, Na; 0.000882, H; 0.01223, O; 0.0435. As the input for the PALLAS one may choose H, O, Si, Ca and Al as

main nuclides in the concrete and use Al and Ca in replacement of respectively Na, Mg, and Fe, which results in nuclear densities of 0.01223, 0.0435, 0.004315, 0.0141, and 0.003704, for H, O, Al, Si, and Ca respectively. Note that the order of nuclides to be inputed is that of identification numbers of the PALLAS library given in Table 2.

(15) Data note 15

All the material regions are numbered as illustrated in Fig.10. In principle at first the numbers 1, 2, ---, 10 are set for (r=1, z=1)-th region, (2,1)-th, ---, (10,1)-th region, and 11, 12, ---, 20 are set for (1,2)-th (2,2)-th, ---, (10,2)-th region, and so on. When the same materials are repeatedly specified in material regions, their identification numbers are replaced by those of the previous same materials as shown in Fig.10.

(16) Data note 16

For IUNCL \neq 0, the unscattered angular flux is analytically calculated at spatial mesh points in specified material regions outside source regions by using the point kernel method based on the angular flux on the surface of the source. The cylindrical volume source is defined using spatial meshes and region numbers as shown in Fig.11. KSR1 is the radial mesh point defining the source radius, and KBR1 is the maximum radial-region number of the source. The top and the bottom mesh numbers are respectively

KZT1 and KZB1, and their region numbers are respectively KBZ1 and KBBZ1. If a source is specified as a symmetry with respect to R axis, $KZT1 > 1$ and $KZB1 \geq 1$ and always $KBZ1 = KBBZ1 = 1$ with $NORF = 0$. In the case of a disk source, $KZT1 = KZB1 = 1$ and also $KBZ1 = KBBZ1 = 1$ when the source is set at $z = 0$ cm. If the source is set at z cm (n -th axial mesh in m -th region), $KZT1 = KBZ1 = n$ and $KZB1 = KBBZ1 = m$.

For a line source, $KZT1 > KBZ1 \geq 1$ and $KZB1 > KBBZ1 \geq 1$ with $KSR1 = KBR1 = 1$, which indicates the line source on z axis. For a point source, $KZT1 = KZB1 \geq 1$ and $KBZ1 = KBBZ1 \geq 1$ with $KSR1 = KBR1 = 1$, which indicates the point source at z cm on z axis.

The angular flux is only one value with respect to radial mesh r_i at $z = z_s$ on a source surface for both a cylindrical source and a disk source because of a symmetry with respect to z axis in (r, z) geometry. For calculation of the unscattered angular fluxes arising from the source surface, the surface must be divided azimuthally into NPFI sections as illustrated in Fig.11. For no specification on NPFI, the code divides equally a half circular area into 4 sections. It is recommended that NPFI is 10 for nearest points to the source surface and 6 ~ 8 for nearer points. For distant points to the source it is adequate to choose 4 for NPFI.

The spatial regions in which the unscattered angular flux calculation is applied are specified as $IUNC(i, j) = 1$. While the regions where only the usual transport calculation is applied are specified as $IUNC(i, j) = 0$.

Note that the nearest spatial region to the source surface

(for instance within 2 ~ 3 cm from the source) should be specified as $IUNC(i,j)=0$. No special caution should be made on a point source. One may specify as $IUNC(i,j)=1$ for all the spatial regions.

(17) Data note 17

As already described in Data note 4, when the parameter IUNCL is minus value, the analytical unscattered flux calculation is made after the usual transport calculation is over at each energy mesh. In this case an assumed source region is newly defined as depicted in Fig.11. The spatial mesh and material-region size indications are same as described in Data note 16. The material regions in which the analytical unscattered flux calculation is executed are specified as $IUNB(i,j)=1$ only outside the assumed source regions, or otherwise $IUNCB(i,j)=0$.

(18) Data note 18

When one wants to replace the total and elastic scattering cross sections taken from the PALLAS neutron library, one may input a certain integer n to ICH. The value n is equal or less than the total energy mesh JJ.

For $n=JJ$, all the total and the elastic scattering cross sections taken are replaced by the new data read in from cards. While $n < JJ$, some of the data are replaced by new data at specified energy meshes. The energy meshes in which the data are replaced are inputted by the parameter LCH(n).

(19) Data note 19

PALLAS code calculates neutron elastic scattering source using the neutron differential scattering cross section. The neutron differential scattering cross section is calculated in the program based on the data of Legendre expansion coefficients $f_{\ell}(E_j)$ given in evaluated nuclear data files such as ENDF/B: First, the scattering distribution function $f(E, \mu)$ is calculated by

$$f(E, \mu) = \sum_{\ell=0}^L \frac{2\ell+1}{4\pi} f_{\ell}(E) P_{\ell}(\mu),$$

where μ is the value of cosine of scattering angle in the center of mass system and L the maximum order given in an evaluated nuclear data file. The maximum number of terms ($L_{\max}=L+1$) is given in Table 3 for each nuclide included in PALLAS library. Then the differential scattering cross section is calculated by

$$\sigma_{el}(\vec{\Omega}' \rightarrow \vec{\Omega}, E' \rightarrow E) = \sigma_{el}(E') f(E', \mu) \delta(\cos\theta - \alpha) \frac{(A+1)^2}{2AE'},$$

where $\sigma_{el}(E)$ is the total elastic scattering cross section, θ and α are respectively the scattering angle and its cosine in the laboratory system, and A the mass of nuclide.

(20) Data note 20

Since the neutrons emitted from $(n, 2n)$ reaction are twice as many as the incident neutrons, the value of each element in the matrix $SN(k, j)$ is doubled in the program and added to the matrix $CIB(k, j)$.

(21) Data note 21

The gamma-ray nuclear data for PALLAS are used as the linear attenuation coefficient of a material. The data of the linear attenuation coefficient may be taken from reports on photon cross sections such as J. H. Hubbell's compiled data.⁸⁾ The scattering cross section should not be entered, because PALLAS can calculate the gamma ray scattering source by directly use of the Klein-Nishina formula.

(22) Data note 22

The parameter KANK is used together with ITP20. Consequently, prior to this use the angular fluxes calculated in advance should be stored in Tape 20. In the case of KANK=1, the angular fluxes stored in Tape 20 are transferred one by one in energy mesh into Disk 10. Let the total energy meshes in the previous calculation be JJ', then the next calculation will start at J(=JJ'+1)-th energy mesh. On the other hand in the case of KANK=2, the coupled neutron calculation explained in Data note 1 is made using Tape 20: For instance first calculation was made with the 0.1 lethargy-width structure and then stored in Tape 20. The angular fluxes stored in Tape 20 are transferred alternatively in energy mesh into Disk 10, i.e. the angular fluxes at energy meshes in odd numbers are transferred into Disk 10. Then the new calculation with the 0.2 lethargy-width structure will start at [(JJ'+3)/2]-th energy mesh, when JJ' is the total number of energy meshes in the previous calculation.

(23) Data note 23

These input data are used for limitation of the output list. If NOR1, NOR2, NOZ1 and NOZ2 are zeros, all the calculated scalar fluxes are printed as an output. If NOR1, NOR2, NOZ1 and NOZ2 > 0, the calculated scalar fluxes are printed at spatial meshes with respect to the r meshes from NOR1-th through NOR2-th and with respect to the z meshes from NOZ1-th through NOZ2-th.

(24) Data note 24

If MRK > 0 and MZK > 0, calculated angular fluxes are printed at the (r,z) spatial meshes defined by the combinations of (KR(n), KZ(n)), n=1, 2, ---, i.e. at (r,z) spatial meshes of (KR(1), KZ(1)), (KR(1), KZ(2)), ---, (KR(1), KZ(MZK)), (KR(2), KZ(1)), ---, (KR(2), KZ(MZK)), ---, (KR(MRK), KZ(1)), ---, (KR(MRK), KZ(MZK)).

Note that PALLAS angular flux is printed in units of $n/cm^2 \cdot sec \cdot sr \cdot MeV$ for IEF=0 and $MeV/cm^2 \cdot sec \cdot sr \cdot MeV$ for IEF=1. In addition PALLAS scalar flux is printed in units of $n/cm^2 \cdot sec \cdot MeV$ for IEF=0 and $MeV/cm^2 \cdot sec \cdot MeV$ or $n/cm^2 \cdot sec \cdot unit$ lethargy for IEF=1. Thermal neutron flux is also printed in units of $n/cm^2 \cdot sec \cdot (sr) \cdot MeV$ for IEF=0. If one wants to obtain thermal neutrons below 0.45 eV or thermal group neutrons below 0.45 eV, one may multiply the thermal neutron flux by 0.45×10^{-6} MeV. On the other hand for IEF=1, thermal neutron flux in units of $n/cm^2 \cdot sec \cdot unit$ lethargy is equal to thermal neutrons below 0.45 eV in units of $n/cm^2 \cdot sec$.

(25) Data note 25

This option is used for such a problem as shown in Fig.12; The first transport calculation is made in ordinary (r,z) geometry, however, the next transport calculation must be made in new (\bar{r},\bar{z}) geometry since a duct is set at the radial direction in original (r,z) geometry. The next transport calculation is made based on the boundary angular flux defined on the surface of the duct mouth. For this purpose the first calculated angular fluxes between LZ1-th and LZ2-th z meshes at LR1=LR2-th r mesh are taken and converted to new boundary angular fluxes in (\bar{r},\bar{z}) geometry.

This option necessitates the other input parameter to store the old angular fluxes in File unit 21; Card-01 ITP21=10 and Card-02 LR1, LR2, LZ1, LZ2.

(26) Additional Data note for energy intervals of gamma-ray calculation

Originally, the energy meshes for gamma-ray calculation are always defined by inputted data. Later the program has been modified so that these values can be defined automatically in it. For this purpose one should define only ΔE by the input HH in units of MeV. Here ΔE is the energy difference with a same energy interval in high energy region (closer to a maximum gamma-ray energy EMAX). This energy-mesh structure, however, is not appropriate for PALLAS gamma-ray calculation, since the wavelength interval defined by the energy mesh interval ΔE becomes too large to calculate accurate gamma-ray transport. For

instance, in the case of EMAX=1 MeV and HH=0.1 MeV, the first four wavelength intervals $\Delta\lambda_j$ ($j=1,2,3,4$) are less than 0.1, however for lower energy meshes such as 0.4, 0.3, and 0.2 MeV these intervals become considerably large such as 0.43 and 0.85. To mitigate such an abrupt increase in wavelength interval the code provides a special definition for the wavelength interval: At first the energy interval determined from ΔE is used down to 2 MeV, and when the energy point becomes less than 2 MeV, the energy interval is defined by using the wavelength interval determined by

$$\Delta\lambda_j = \Delta\lambda_{j-1} \times 1.2.$$

When thus determined $\Delta\lambda_j$ is over than 0.4, the wavelength interval is redetermined by

$$\Delta\lambda_j = \Delta\lambda_{j-1} \times 1.1.$$

However, when thus defined $\Delta\lambda_j$ is over than 0.45, the value of $\Delta\lambda_j$ is fixed as approximately $0.45 \sim 0.49$.

Example for 3.25 MeV and HH=0.5 MeV.

No.	E_j	λ_j	$\Delta\lambda_j$
1	3.25	0.1572	0.0143
2	2.75	0.1858	0.0349
3	2.25	0.227	0.0531
4	1.75	0.292	0.0714
5	1.382	0.370	0.08565
6	1.103	0.463	0.1028
7	0.888	0.575	0.1233

8	0.720	0.710	0.148
9	0.586	0.872	0.1776
10	0.480	1.065	0.2131
11	0.394	1.298	0.2558
12	0.324	1.577	0.3069
13	0.267	1.912	0.3516
14	0.224	2.28	0.3867
15	0.190	2.685	0.4254
16	0.1632	3.131	0.4902
17	0.141	3.624	0.4902
18	0.124	4.121	0.4902
19	0.111	4.604	0.4902
20	0.100	5.11	0.4902

3.3 External and internal data files

All the files used for input, output and scratched data are given in Table 5. All the PALLAS calculations need always file units 2, 3, 5, 6, 8, 10, and 14. For neutron transport calculations the PALLAS neutron library is required, while the PALLAS gamma-ray library is fixed at file unit 31. The file unit 12 is always necessary for neutron transport calculations. When one uses the analytical unscattered-flux calculation option one must prepare file unit 15, and when one uses the boundary angular fluxes for transport calculations one must prepare file unit 11 and/or unit 17 or unit 18.

If the parameter $ITP29 > 0$, file units 19 and 29 must be prepared so that calculated scalar fluxes stored in the file unit 19 can be transferred to the file unit 29 for keeping.

3.4 Program mnemonics and program variables

Relation of main variables used in the code to program mnemonics is given in Table 6. Additional important variables are radial distances (in cm) at m-th meshes ($m=1, 2, \dots, MRR$) and also axial distances (in cm) at n-th meshes ($n=1, 2, \dots, MZZ$), which are represented as $RNEW(M)$ and $ZD(N)$ in the program mnemonics.

3.5 Sample problems

(1) Sample problem 1: Neutron cylindrical volume source problem with a fission source

The input data for this problem are shown in Fig.16-1 ~ -3. Since KIN=2, coupled neutron calculations are carried out with 0.1-, 0.2- and 0.4- lethargy structures. First, the input data for a calculation with 0.1-lethargy structure are specified from No.3 through No.55, and successively those for a calculation with 0.2-lethargy structure are specified from No.56 through No.105, and those for a calculation with 0.4-lethargy structure are specified from No.106 to the last card.

The list of the input data for the calculation with 0.1-lethargy structure is shown in Fig.16-4 ~ -6, in which the neutron energy meshes are defined for 0.1 lethargy intervals and the angular quadrature and weight are also defined together with azimuthal angular meshes in the code. In spite of three types of reaction cross sections inputted, four reactions are used as given in Fig.16-6. The reason is to calculate always the dose equivalent rate (mrem/h) in the code.

(2) Sample problem 2: Gamma-ray room scattering problem for a point continuous energy source

The input data for this problem are shown in Fig.17-1 ~ -2. The energy mesh points are inputted as specified in No.11 ~ No.14 since the input HH=0.0. The minus signs of NOEL indicate that both linear attenuation coefficients and pair production

coefficients are read in from input cards. The zeros of NEK indicate void regions through which gamma rays stream into a concrete-wall room.

The list of the input data is shown in Fig.17-3 ~ -5, in which the wavelengths and their intervals are also printed as WAVE(J) and DWAVE(J). The point isotropic source position is all "1". The input IUNC=1 for all the material regions, which indicates that the analytical unscattered flux calculation is carried out in all the regions. The last of the list is the dose conversion factor, which is always utilized for gamma-ray calculations.

(3) Sample problem 3: Monoenergy gamma-ray volume source problem

The input data for this problem are shown in Fig.18. The input MONOE=10 for ^{137}Cs gamma-ray source. The energy mesh points are defined in the code based on the input HH=0.04 (MeV).

The input ITP21=10 is specified in NO.29, which requires Card-02. Consequently the input LR1, LR2, LZ1 and LZ2 are prepared in No.30, which indicates that angular fluxes to be calculated are picked up at radial meshes 1 through 30 at 30-th axial mesh to store in File unit 21.

(4) Sample problem 4: Gamma-ray skyshine problem

This is an example of a gamma-ray skyshine problem: The gamma rays streaming through the ceiling of a water-pool facility are calculated in Sample problem 3 and the angular fluxes at the

height of the ceiling are stored in File unit 21. Consequently the sample 4 is calculated based on the angular fluxes in File unit 21, which requires to input 10 for NBND and 22 for LTAP as shown in No.4 of Fig.19-1. The input IUNCL=25 indicates that the analytical unscattered flux calculation is executed up to 25-th energy mesh, which requires the specification of the source region as given in No.23.

The list of the input data is provided in Fig.19-2 ~ -3. The angular fluxes are read from J=1 through J=31 energy mesh from File unit 22, which become the boundary angular fluxes at each energy mesh.

(5) Sample problem 5: Neutron flux estimation within a space behind a shield with a straight duct

The input data are shown in Fig.20-1 ~ -3. This problem is a neutron streaming through a straight air duct for the mono-energy 14-MeV neutron source assumed as a disk source. There is a large space or room behind the shield, so that scattered neutrons within the duct and penetrated neutrons in addition to the streaming neutrons cause the increase of the neutron dose level within the space. For estimation of the neutron flux in the large space, one should input the negative integer (-25) for IUNCL, which indicates that neutron streaming and penetration calculations are carried out using the analytical unscattered flux calculation option at each energy mesh and after that the additional analytical unscattered flux calculation is also

carried out in the space using thus evaluated angular fluxes on the back surface of the shield at each energy mesh. Since the source of the sample problem is the monoenergy source, the analytical unscattered flux calculation is executed only once for the monoenergy source. Consequently the input data for specifying the material regions, $IUNC(i,j)$, are all zeros for 0.2- and 0.4-lethargy interval structures.

The list of the input data is provided in Fig.20-4 ~ -5, in which the boundary angular fluxes are all the same values of $1/2\pi$ on the disk source for the first energy mesh. The streaming region is specified as zeros for both NOEL and NEK.

3.6 Other note

Since no iterative calculations are applied in the PALLAS code for estimation of within-group scattered radiations, it should be essentially required to use fine energy meshes in neutron deep penetration calculations in material regions composed of large mass numbers such as sodium, iron or lead. Although it is ideal to apply so fine energy meshes that at least a few energy meshes can be chosen within the maximum energy degradation, practical calculations choose rather rough energy meshes, which results in sometimes considerable calculational errors. One of mitigations of the errors is to apply the weighting function option (IRWRT>0) to assume the rising gradient of the spectra in thick material regions. In addition, it should be essential to use region-wise effective cross sections that can be processed by one-dimensional transport calculations with ultra-fine energy meshes.

4. ANGULAR MESH POINTS AND NUCLEAR DATA USED IN PALLAS CODE

4.1 Angular mesh points

The angular variable $\bar{\Omega}$ is represented by discrete-ordinate directional points $\bar{\Omega}_{pq} (= \bar{\Omega}(\theta_p, \phi_{pq}))$ on a unit sphere, where the θ is the polar angle and the ϕ is the azimuthal angle as shown in Figs.14 and 15. In PALLAS calculation, $\omega = \cos\theta$ is used instead of θ . The values for $\bar{\Omega}_{pq}(\omega_p, \phi_{pq})$ fixed in the present code are given under Fig.15 for $p \leq 4$, since the angular points are distributed symmetrically with respect to the r axis as shown in Fig.15. Basically any constants can be used for the PALLAS angular quadrature set. The present constants have been calculated in the following manner: First, the center point in each ω_p -range governed by its weight was chosen as the value for ω_p . Second, the center point in each ϕ_{pq} -range governed by its weight was also chosen as the value for ϕ_{pq} , and then the weight for each $\bar{\Omega}_{pq}$ was determined with multiplying the ω_p -weight by the ϕ_{pq} -weight.

One may use the other angular quadrature sets defined under the restriction of the total 28 mesh points symmetrical with respect to the r axis.

4.2 Nuclear data for PALLAS

As already mentioned, PALLAS calculates radiation scattering as precisely as possible. For gamma ray scattering the Klein-Nishina formula is directly utilized so that PALLAS calculated

angular flux can represent precisely physical phenomena. Then no gamma-ray scattering data are necessary.

For neutron nuclear data the infinite dilution point energy data have been prepared in PALLAS INF-series library,⁹⁾ in which the total cross sections σ_t , σ_c and σ_{el} at all the energy points written in ENDF/B-IV data file were averaged in the energy intervals defined in Table 1. The weighting function for averaging was fission $+1/E$ spectrum. All the Legendre expansion coefficients given in ENDF/B-IV file were used for obtaining, those at the energy meshes in PALLAS library defined in Table 1. The inelastic slowing down matrix were prepared with use of SUPERTOG code.¹⁰⁾

The effective cross sections used in practical PALLAS calculations have been prepared in PALLAS EFF-series library, for each nuclide provided in Table 1. For any mixtures one must determine the self-shielding factor for these mixtures by oneself.

REFERENCES

- 1) Takeuchi K.: "Numerical Solution to Space-Angle Energy Dependent Neutron Integral Transport Equation", J. Nucl. Sci. Technol., Vol.8 No.3 (1971).
- 2) Takeuchi K. and Sasamoto N.: "Fundamental Theory of the Direct Integration Method for Solving the Steady-State Integral Transport Equation for Radiation Shielding Calculation", Nucl. Sci. Eng., 80, 536 (1982).
- 3) Sasamoto N. and Takeuchi K.: "Analysis of ^{60}Co Gamma-Ray Transport Through Air by Discrete-Ordinates Transport Codes", Nucl. Tech. Vol.47 (1), . 89 (1980).
- 4) Sasamoto N. and Takeuchi K.: "An Improvement of the PALLAS Discrete-Ordinates Transport Code", Nucl. Sci. Eng. 71, 330 (1979).
- 5) Takeuchi K.: "PALLAS-2DCY, A Two-Dimensional Transport Code", Papers Ship Res. Inst. No.47 (1973).
- 6) Takeuchi K.: "PALLAS-@DCY: A Code for Direct Integraon of Transport Equation in Two-Dimensional (R,Z) Geometry", JAERI-M 9014 (1980).
- 7) Takeuchi K.: "PALLAS-2DCY-FC, A Computational method and Radiation Transport Code in Two-Dimensional (R,Z) Geometry", Papers Ship Res. Inst. No.57 (1979)
- 8) Hubbell J.H.: "Photon Cross Sections, Attenuation Codfficients, and Energy Absorption Coefficients From 10 KeV to 100 GeV", NSRDS-NBS 29 (1969).
- 9) Sasamoto N. and Takeuchi K.: "Revision of Multi-group Neutron Cross Section Libraries for P LLAS", JAERI-M 9527 (1981).

- 10) Wright R.Q., et al.: "SUPERTOG: A Program to Generate Fine Group Constants and Pn Scattering Matrices From ENDF/B", ORNL-TM-2679 (1969).

Table 1 Energy mesh structures used in PALLAS neutron library
Lethargy-width structures of 0.05, 0.1, 0.2 and 0.4
are given.

0.05 LETHARGY WIDTH STRUCTURE

GROUP	ENERGY MESH (EV)	UPPER BOUND. (EV)	LOWER BOUND. (EV)
1	1.4200E+07	1.4559E+07	1.3849E+07
2	1.3507E+07	1.3849E+07	1.3174E+07
3	1.2849E+07	1.3174E+07	1.2531E+07
4	1.2222E+07	1.2531E+07	1.1920E+07
5	1.1626E+07	1.1920E+07	1.1339E+07
6	1.1059E+07	1.1339E+07	1.0786E+07
7	1.0520E+07	1.0786E+07	1.0260E+07
8	1.0007E+07	1.0260E+07	9.7595E+06
9	9.5185E+06	9.7595E+06	9.2835E+06
10	9.0543E+06	9.2835E+06	8.8308E+06
11	8.6127E+06	8.8308E+06	8.4001E+06
12	8.1927E+06	8.4001E+06	7.9904E+06
13	7.7931E+06	7.9904E+06	7.6007E+06
14	7.4131E+06	7.6007E+06	7.2300E+06
15	7.0515E+06	7.2300E+06	6.8774E+06
16	6.7076E+06	6.8774E+06	6.5420E+06
17	6.3805E+06	6.5420E+06	6.2229E+06
18	6.0693E+06	6.2229E+06	5.9194E+06
19	5.7733E+06	5.9194E+06	5.6307E+06
20	5.4917E+06	5.6307E+06	5.3561E+06
21	5.2239E+06	5.3561E+06	5.0949E+06
22	4.9691E+06	5.0949E+06	4.8464E+06
23	4.7268E+06	4.8464E+06	4.6101E+06
24	4.4962E+06	4.6101E+06	4.3852E+06
25	4.2770E+06	4.3852E+06	4.1714E+06
26	4.0684E+06	4.1714E+06	3.9679E+06
27	3.8700E+06	3.9679E+06	3.7744E+06
28	3.6812E+06	3.7744E+06	3.5903E+06
29	3.5017E+06	3.5903E+06	3.4152E+06
30	3.3309E+06	3.4152E+06	3.2487E+06
31	3.1684E+06	3.2487E+06	3.0902E+06
32	3.0139E+06	3.0902E+06	2.9395E+06
33	2.8669E+06	2.9395E+06	2.7961E+06
34	2.7271E+06	2.7961E+06	2.6598E+06
35	2.5941E+06	2.6598E+06	2.5301E+06
36	2.4676E+06	2.5301E+06	2.4067E+06
37	2.3472E+06	2.4067E+06	2.2893E+06
38	2.2328E+06	2.2893E+06	2.1776E+06
39	2.1239E+06	2.1776E+06	2.0714E+06
40	2.0203E+06	2.0714E+06	1.9704E+06
41	1.9218E+06	1.9704E+06	1.8743E+06
42	1.8280E+06	1.8743E+06	1.7829E+06
43	1.7389E+06	1.7829E+06	1.6959E+06
44	1.6541E+06	1.6959E+06	1.6132E+06
45	1.5734E+06	1.6132E+06	1.5346E+06
46	1.4967E+06	1.5346E+06	1.4597E+06
47	1.4237E+06	1.4597E+06	1.3885E+06
48	1.3542E+06	1.3885E+06	1.3208E+06
49	1.2882E+06	1.3208E+06	1.2564E+06
50	1.2254E+06	1.2564E+06	1.1951E+06

Table 1 (continued)

51	1.1656E+06	1.1951E+06	1.1368E+06
52	1.1088E+06	1.1368E+06	1.0814E+06
53	1.0547E+06	1.0814E+06	1.0286E+06
54	1.0032E+06	1.0286E+06	9.7848E+05
55	9.5432E+05	9.7848E+05	9.3076E+05
56	9.0778E+05	9.3076E+05	8.8536E+05
57	8.6350E+05	8.8536E+05	8.4218E+05
58	8.2139E+05	8.4218E+05	8.0111E+05
59	7.8133E+05	8.0111E+05	7.6204E+05
60	7.4322E+05	7.6204E+05	7.2487E+05
61	7.0698E+05	7.2487E+05	6.8952E+05
62	6.7250E+05	6.8952E+05	6.5589E+05
63	6.3970E+05	6.5589E+05	6.2390E+05
64	6.0850E+05	6.2390E+05	5.9348E+05
65	5.7882E+05	5.9348E+05	5.6453E+05
66	5.5059E+05	5.6453E+05	5.3700E+05
67	5.2374E+05	5.3700E+05	5.1081E+05
68	4.9820E+05	5.1081E+05	4.8590E+05
69	4.7390E+05	4.8590E+05	4.6220E+05
70	4.5079E+05	4.6220E+05	4.3966E+05
71	4.2880E+05	4.3966E+05	4.1822E+05
72	4.0789E+05	4.1822E+05	3.9782E+05
73	3.8800E+05	3.9782E+05	3.7842E+05
74	3.6907E+05	3.7842E+05	3.5996E+05
75	3.5107E+05	3.5996E+05	3.4241E+05
76	3.3395E+05	3.4241E+05	3.2571E+05
77	3.1767E+05	3.2571E+05	3.0982E+05
78	3.0217E+05	3.0982E+05	2.9471E+05
79	2.8744E+05	2.9471E+05	2.8034E+05
80	2.7342E+05	2.8034E+05	2.6667E+05
81	2.6008E+05	2.6667E+05	2.5366E+05
82	2.4740E+05	2.5366E+05	2.4129E+05
83	2.3533E+05	2.4129E+05	2.2952E+05
84	2.2385E+05	2.2952E+05	2.1833E+05
85	2.1294E+05	2.1833E+05	2.0768E+05
86	2.0255E+05	2.0768E+05	1.9755E+05
87	1.9267E+05	1.9755E+05	1.8792E+05
88	1.8328E+05	1.8792E+05	1.7875E+05
89	1.7434E+05	1.7875E+05	1.7003E+05
90	1.6584E+05	1.7003E+05	1.6174E+05
91	1.5775E+05	1.6174E+05	1.5385E+05
92	1.5005E+05	1.5385E+05	1.4635E+05
93	1.4274E+05	1.4635E+05	1.3921E+05
94	1.3577E+05	1.3921E+05	1.3242E+05
95	1.2915E+05	1.3242E+05	1.2596E+05
96	1.2285E+05	1.2596E+05	1.1982E+05
97	1.1686E+05	1.1982E+05	1.1398E+05
98	1.1116E+05	1.1398E+05	1.0842E+05
99	1.0574E+05	1.0842E+05	1.0313E+05
100	1.0058E+05	1.0313E+05	9.8101E+04

Table 1 (continued)

0.1 LETHARGY WIDTH STRUCTURE

GROUP	ENERGY MESH (EV)	UPPER BOUND. (EV)	LOWER BOUND. (EV)
1	1.4200E+07	1.4928E+07	1.3507E+07
2	1.2849E+07	1.3507E+07	1.2222E+07
3	1.1626E+07	1.2222E+07	1.1059E+07
4	1.0520E+07	1.1059E+07	1.0007E+07
5	9.5185E+06	1.0007E+07	9.0543E+06
6	8.6127E+06	9.0543E+06	8.1927E+06
7	7.7931E+06	8.1927E+06	7.4130E+06
8	7.0515E+06	7.4131E+06	6.7076E+06
9	6.3805E+06	6.7076E+06	6.0693E+06
10	5.7733E+06	6.0693E+06	5.4917E+06
11	5.2239E+06	5.4917E+06	4.9691E+06
12	4.7268E+06	4.9691E+06	4.4962E+06
13	4.2770E+06	4.4962E+06	4.0684E+06
14	3.8700E+06	4.0684E+06	3.6812E+06
15	3.5017E+06	3.6812E+06	3.3309E+06
16	3.1684E+06	3.3309E+06	3.0139E+06
17	2.8669E+06	3.0139E+06	2.7271E+06
18	2.5941E+06	2.7271E+06	2.4676E+06
19	2.3472E+06	2.4676E+06	2.2328E+06
20	2.1239E+06	2.2328E+06	2.0203E+06
21	1.9218E+06	2.0203E+06	1.8280E+06
22	1.7389E+06	1.8280E+06	1.6541E+06
23	1.5734E+06	1.6541E+06	1.4967E+06
24	1.4237E+06	1.4967E+06	1.3542E+06
25	1.2882E+06	1.3542E+06	1.2254E+06
26	1.1656E+06	1.2254E+06	1.1088E+06
27	1.0547E+06	1.1088E+06	1.0032E+06
28	9.5432E+05	1.0032E+06	9.0778E+05
29	8.6350E+05	9.0778E+05	8.2139E+05
30	7.8133E+05	8.2139E+05	7.4322E+05
31	7.0698E+05	7.4322E+05	6.7250E+05
32	6.3970E+05	6.7250E+05	6.0850E+05
33	5.7882E+05	6.0850E+05	5.5059E+05
34	5.2374E+05	5.5059E+05	4.9820E+05
35	4.7390E+05	4.9820E+05	4.5079E+05
36	4.2880E+05	4.5079E+05	4.0789E+05
37	3.8800E+05	4.0789E+05	3.6907E+05
38	3.5107E+05	3.6907E+05	3.3395E+05
39	3.1766E+05	3.3395E+05	3.0217E+05
40	2.8743E+05	3.0217E+05	2.7342E+05
41	2.6008E+05	2.7342E+05	2.4740E+05
42	2.3533E+05	2.4740E+05	2.2385E+05
43	2.1294E+05	2.2385E+05	2.0255E+05
44	1.9267E+05	2.0255E+05	1.8328E+05
45	1.7434E+05	1.8328E+05	1.6584E+05
46	1.5775E+05	1.6584E+05	1.5005E+05
47	1.4274E+05	1.5005E+05	1.3577E+05
48	1.2915E+05	1.3577E+05	1.2285E+05
49	1.1686E+05	1.2285E+05	1.1116E+05
50	1.0574E+05	1.1116E+05	1.0058E+05

Table 1 (continued)

51	9.5679E+04	1.0058E+05	9.1012E+04
52	8.6574E+04	9.1013E+04	8.2351E+04
53	7.8335E+04	8.2351E+04	7.4515E+04
54	7.0881E+04	7.4515E+04	6.7424E+04
55	6.4135E+04	6.7424E+04	6.1007E+04
56	5.8032E+04	6.1007E+04	5.5202E+04
57	5.2510E+04	5.5202E+04	4.9949E+04
58	4.7513E+04	4.9949E+04	4.5195E+04
59	4.2991E+04	4.5195E+04	4.0895E+04
60	3.8900E+04	4.0895E+04	3.7003E+04
61	3.5198E+04	3.7003E+04	3.3482E+04
62	3.1849E+04	3.3482E+04	3.0295E+04
63	2.8818E+04	3.0295E+04	2.7412E+04
64	2.6075E+04	2.7412E+04	2.4804E+04
65	2.3594E+04	2.4804E+04	2.2443E+04
66	2.1349E+04	2.2443E+04	2.0308E+04
67	1.9317E+04	2.0308E+04	1.8375E+04
68	1.7479E+04	1.8375E+04	1.6626E+04
69	1.5816E+04	1.6626E+04	1.5044E+04
70	1.4311E+04	1.5044E+04	1.3613E+04
71	1.2949E+04	1.3613E+04	1.2317E+04
72	1.1716E+04	1.2317E+04	1.1145E+04
73	1.0601E+04	1.1145E+04	1.0084E+04
74	9.5926E+03	1.0084E+04	9.1248E+03
75	8.6798E+03	9.1248E+03	8.2565E+03
76	7.8538E+03	8.2565E+03	7.4708E+03
77	7.1064E+03	7.4708E+03	6.7598E+03
78	6.4301E+03	6.7598E+03	6.1165E+03
79	5.8182E+03	6.1165E+03	5.5345E+03
80	5.2645E+03	5.5345E+03	5.0078E+03
81	4.7636E+03	5.0078E+03	4.5312E+03
82	4.3102E+03	4.5312E+03	4.1000E+03
83	3.9001E+03	4.1000E+03	3.7099E+03
84	3.5289E+03	3.7099E+03	3.3568E+03
85	3.1931E+03	3.3568E+03	3.0374E+03
86	2.8892E+03	3.0374E+03	2.7483E+03
87	2.6143E+03	2.7483E+03	2.4868E+03
88	2.3655E+03	2.4868E+03	2.2501E+03
89	2.1404E+03	2.2501E+03	2.0360E+03
90	1.9367E+03	2.0360E+03	1.8423E+03
91	1.7524E+03	1.8423E+03	1.6669E+03
92	1.5857E+03	1.6670E+03	1.5083E+03
93	1.4348E+03	1.5083E+03	1.3648E+03
94	1.2982E+03	1.3648E+03	1.2349E+03
95	1.1747E+03	1.2349E+03	1.1174E+03
96	1.0629E+03	1.1174E+03	1.0111E+03
97	9.6175E+02	1.0111E+03	9.1484E+02
98	8.7022E+02	9.1484E+02	8.2778E+02
99	7.8741E+02	8.2778E+02	7.4901E+02
100	7.1248E+02	7.4901E+02	6.7773E+02

Table 1 (continued)

0.2 LETHARGY WIDTH STRUCTURE

GROUP	ENERGY MESH (EV)	UPPER BOUND. (EV)	LOWER BOUND. (EV)
1	1.4200E+07	1.5693E+07	1.2849E+07
2	1.1626E+07	1.2849E+07	1.0520E+07
3	9.5185E+06	1.0520E+07	8.6127E+06
4	7.7931E+06	8.6127E+06	7.0515E+06
5	6.3805E+06	7.0515E+06	5.7733E+06
6	5.2239E+06	5.7733E+06	4.7268E+06
7	4.2770E+06	4.7268E+06	3.8700E+06
8	3.5017E+06	3.8700E+06	3.1684E+06
9	2.8669E+06	3.1685E+06	2.5941E+06
10	2.3472E+06	2.5941E+06	2.1239E+06
11	1.9218E+06	2.1239E+06	1.7389E+06
12	1.5734E+06	1.7389E+06	1.4237E+06
13	1.2882E+06	1.4237E+06	1.1656E+06
14	1.0547E+06	1.1656E+06	9.5432E+05
15	8.6350E+05	9.5432E+05	7.8133E+05
16	7.0698E+05	7.8133E+05	6.3970E+05
17	5.7882E+05	6.3970E+05	5.2374E+05
18	4.7390E+05	5.2374E+05	4.2880E+05
19	3.8800E+05	4.2880E+05	3.5107E+05
20	3.1767E+05	3.5107E+05	2.8744E+05
21	2.6008E+05	2.8744E+05	2.3533E+05
22	2.1294E+05	2.3533E+05	1.9267E+05
23	1.7434E+05	1.9267E+05	1.5775E+05
24	1.4274E+05	1.5775E+05	1.2915E+05
25	1.1686E+05	1.2915E+05	1.0574E+05
26	9.5679E+04	1.0574E+05	8.6574E+04
27	7.8335E+04	8.6574E+04	7.0881E+04
28	6.4135E+04	7.0881E+04	5.8032E+04
29	5.2510E+04	5.8032E+04	4.7513E+04
30	4.2991E+04	4.7513E+04	3.8900E+04
31	3.5198E+04	3.8900E+04	3.1849E+04
32	2.8818E+04	3.1849E+04	2.6076E+04
33	2.3594E+04	2.6076E+04	2.1349E+04
34	1.9317E+04	2.1349E+04	1.7479E+04
35	1.5816E+04	1.7479E+04	1.4311E+04
36	1.2949E+04	1.4311E+04	1.1717E+04
37	1.0602E+04	1.1717E+04	9.5927E+03
38	8.6798E+03	9.5927E+03	7.8538E+03
39	7.1064E+03	7.8538E+03	6.4301E+03
40	5.8182E+03	6.4302E+03	5.2646E+03
41	4.7636E+03	5.2646E+03	4.3103E+03
42	3.9001E+03	4.3103E+03	3.5289E+03
43	3.1931E+03	3.5289E+03	2.8893E+03
44	2.6143E+03	2.8893E+03	2.3655E+03
45	2.1404E+03	2.3655E+03	1.9367E+03
46	1.7524E+03	1.9367E+03	1.5857E+03
47	1.4348E+03	1.5857E+03	1.2982E+03
48	1.1747E+03	1.2982E+03	1.0629E+03
49	9.6175E+02	1.0629E+03	8.7023E+02
50	7.8741E+02	8.7023E+02	7.1248E+02

Table 1 (continued)

51	6.4468E+02	7.1248E+02	5.8333E+02
52	5.2782E+02	5.8333E+02	4.7759E+02
53	4.3214E+02	4.7759E+02	3.9102E+02
54	3.5381E+02	3.9102E+02	3.2014E+02
55	2.8967E+02	3.2014E+02	2.6211E+02
56	2.3716E+02	2.6211E+02	2.1460E+02
57	1.9417E+02	2.1460E+02	1.7570E+02
58	1.5898E+02	1.7570E+02	1.4385E+02
59	1.3016E+02	1.4385E+02	1.1777E+02
60	1.0656E+02	1.1777E+02	9.6424E+01
61	8.7248E+01	9.6424E+01	7.8945E+01
62	7.1433E+01	7.8945E+01	6.4635E+01
63	5.8484E+01	6.4635E+01	5.2919E+01
64	4.7883E+01	5.2919E+01	4.3326E+01
65	3.9203E+01	4.3326E+01	3.5472E+01
66	3.2097E+01	3.5472E+01	2.9042E+01
67	2.6279E+01	2.9042E+01	2.3778E+01
68	2.1515E+01	2.3778E+01	1.9468E+01
69	1.7615E+01	1.9468E+01	1.5939E+01
70	1.4422E+01	1.5939E+01	1.3050E+01
71	1.1808E+01	1.3050E+01	1.0684E+01
72	9.6673E+00	1.0684E+01	8.7474E+00
73	7.9150E+00	8.7474E+00	7.1617E+00
74	6.4802E+00	7.1617E+00	5.8635E+00
75	5.3056E+00	5.8635E+00	4.8007E+00
76	4.3438E+00	4.8007E+00	3.9304E+00
77	3.5564E+00	3.9304E+00	3.2180E+00
78	2.9117E+00	3.2180E+00	2.6347E+00
79	2.3839E+00	2.6347E+00	2.1571E+00
80	1.9518E+00	2.1571E+00	1.7661E+00
81	1.5980E+00	1.7661E+00	1.4459E+00
82	1.3083E+00	1.4459E+00	1.1838E+00
83	1.0712E+00	1.1838E+00	9.6924E-01
84	8.7701E-01	9.6924E-01	7.9355E-01
85	7.1804E-01	7.9355E-01	6.4971E-01
86	5.8788E-01	6.4971E-01	5.3194E-01
87	4.8131E-01	5.3193E-01	4.3551E-01
88	3.9406E-01	4.3551E-01	0.0

Table 1 (continued)

0.4 LETHARGY WIDTH STRUCTURE

GROUP	ENERGY MESH (EV)	UPPER BOUND. (EV)	LOWER BOUND. (EV)
1	1.4200E+07	1.7344E+07	1.1626E+07
2	9.5185E+06	1.1626E+07	7.7931E+06
3	6.3805E+06	7.7931E+06	5.2239E+06
4	4.2770E+06	5.2239E+06	3.5017E+06
5	2.8669E+06	3.5017E+06	2.3472E+06
6	1.9218E+06	2.3472E+06	1.5734E+06
7	1.2882E+06	1.5734E+06	1.0547E+06
8	8.6350E+05	1.0547E+06	7.0698E+05
9	5.7882E+05	7.0698E+05	4.7390E+05
10	3.8800E+05	4.7390E+05	3.1767E+05
11	2.6008E+05	3.1767E+05	2.1294E+05
12	1.7434E+05	2.1294E+05	1.4274E+05
13	1.1686E+05	1.4274E+05	9.5679E+04
14	7.8335E+04	9.5679E+04	6.4136E+04
15	5.2510E+04	6.4135E+04	4.2991E+04
16	3.5198E+04	4.2991E+04	2.8818E+04
17	2.3594E+04	2.8818E+04	1.9317E+04
18	1.5816E+04	1.9317E+04	1.2949E+04
19	1.0602E+04	1.2949E+04	8.6798E+03
20	7.1064E+03	8.6798E+03	5.8182E+03
21	4.7636E+03	5.8182E+03	3.9001E+03
22	3.1931E+03	3.9001E+03	2.6143E+03
23	2.1404E+03	2.6143E+03	1.7524E+03
24	1.4348E+03	1.7524E+03	1.1747E+03
25	9.6175E+02	1.1747E+03	7.8741E+02
26	6.4468E+02	7.8741E+02	5.2782E+02
27	4.3214E+02	5.2782E+02	3.5381E+02
28	2.8967E+02	3.5381E+02	2.3716E+02
29	1.9417E+02	2.3716E+02	1.5898E+02
30	1.3016E+02	1.5898E+02	1.0656E+02
31	8.7248E+01	1.0656E+02	7.1433E+01
32	5.8484E+01	7.1433E+01	4.7883E+01
33	3.9203E+01	4.7883E+01	3.2097E+01
34	2.6279E+01	3.2097E+01	2.1515E+01
35	1.7615E+01	2.1515E+01	1.4422E+01
36	1.1808E+01	1.4422E+01	9.6673E+00
37	7.9150E+00	9.6673E+00	6.4802E+00
38	5.3056E+00	6.4802E+00	4.3438E+00
39	3.5564E+00	4.3438E+00	2.9117E+00
40	2.3839E+00	2.9117E+00	1.9518E+00
41	1.5980E+00	1.9518E+00	1.3083E+00
42	1.0712E+00	1.3083E+00	8.7701E-01
43	7.1804E-01	8.7701E-01	5.8788E-01
44	4.8131E-01	5.8787E-01	3.9406E-01
45	3.2263E-01	3.9407E-01	0.0

Table 1

(continued)

Group	0.8 Lethargy width structure		
	E_g (eV)	E_{up} (eV)	E_{lw} (eV)
1	1.4208 E+07	1.9607 E+07	8.8099 E+06
2	6.3842 E+06	8.8099 E+06	3.9586 E+06
3	2.8686 E+06	3.9586 E+06	1.7787 E+06
4	1.2890 E+06	1.7787 E+06	7.9922 E+05
5	5.7917 E+05	7.9922 E+05	3.5911 E+05
6	2.6024 E+05	3.5911 E+05	1.6136 E+05
7	1.1693 E+05	1.6136 E+05	7.2504 E+04
8	5.2541 E+04	7.2504 E+04	3.2578 E+04
9	2.3608 E+04	3.2578 E+04	1.4638 E+04
10	1.0608 E+04	1.4638 E+04	6.5774 E+03
11	4.7664 E+03	6.5774 E+03	2.9554 E+03
12	2.1417 E+03	2.9554 E+03	1.3279 E+03
13	9.6232 E+02	1.3279 E+03	5.9669 E+02
14	4.3240 E+02	5.9669 E+02	2.6811 E+02
15	1.9429 E+02	2.6811 E+02	1.2047 E+02
16	8.7299 E+01	1.2047 E+02	5.4130 E+01
17	3.9226 E+01	5.4130 E+01	2.4322 E+01
18	1.7629 E+01	2.4322 E+01	1.0929 E+01
19	7.9196 E+00	1.0929 E+01	4.9106 E+00
20	3.5585 E+00	4.9106 E+00	2.2065 E+00
21	1.5989 E+00	2.2065 E+00	9.9143 E-01
22	7.1845 E-01	9.9143 E-01	4.4548 E-01
23	3.2281 E-01	4.4548 E-01	2.0017 E-01

Table 2 List of identification numbers of nuclides used
in PALLAS neutron and gamma-ray libraries

No.	Nuclide	Identification Number				
		$\Delta u=0.05$	$\Delta u=0.1$	$\Delta u=0.2$	$\Delta u=0.4$	$\Delta u=0.8$
1	H-1	5011	1011	2011	4011	8011
2	H-2	5012	1012	2012	4012	8012
3	Li-6	5036	1036	2036	4036	8036
4	Li-7	5037	1037	2037	4037	8037
5	Be-9	5039	1039	2039	4039	8039
6	B-10	5050	1050	2050	4050	8050
7	B-11	5051	1051	2051	4051	8051
8	C-12	5062	1062	2062	4062	8062
9	N-14	5074	1074	2074	4074	8074
10	O-16	5086	1086	2086	4086	8086
11	F	5090	1090	2090	4090	8090
12	Na-23	5113	1113	2113	4113	8113
13	Mg	5120	1120	2120	4120	8120
14	Al-27	5137	1137	2137	4137	8137
15	Si	5140	1140	2140	4140	8140
16	Ca	5200	1200	2200	4200	8200
17	Cr	5240	1240	2240	4240	8240
18	Mn-55	5255	1255	2255	4255	8255
19	Fe	5260	1260	2260	4260	8260
20	Ni	5280	1280	2280	4280	8280
21	Cu	5290	1290	2290	4290	8290
22	Zr	5400	1400	2400	4400	8400
23	Mo	5420	1420	2420	4420	8420
24	W	5740	1740	2740	4740	8740
25	Pb	5820	1820	2820	4820	8820
26	U-235	5925	1925	2925	4925	8925
27	U-238	5928	1928	2928	4928	8928
28	SUS(304)	5500	1500	2500	4500	8500
29	SUS(316)	5510	1510	2510	4510	8510
30	Ordinary Concrete	5520	1520	2520	4520	8520
31	Heavy Concrete	5530	1530	2530	4530	8530

Table 2 (supplement)

No.	Materials	Identification Number for photon data*
32	Water	540
33	Air	550

* For only photon data (KNDG=4), two materials are identified by three digits in Card 21.

Table 3 Maximum number of terms of Legendre polynomials and the energy group number and the corresponding energy above which the anisotropy of elastic scattering is taken into account.¹⁾

Nuclide	$L_{\max}^{*)}$	$\Delta u=0.1$		$\Delta u=0.2$		$\Delta u=0.4$		$\Delta u=0.8$	
		Grp. ^{**)}	$E_n^{**)}$ (eV)	Grp.	E_n (eV)	Grp.	E_n (eV)	Grp.	E_n (eV)
H-1	1	0	1.42+7 ¹⁾	0	1.42+7	0	1.42+7	0	1.42+7
Li-6	9	50	1.06+4	37	1.06+4	19	1.06+4	10	1.06+4
Li-7	10	43	2.13+5	22	2.13+5	11	2.60+5	6	2.60+5
B-10	9	46	1.58+5	23	1.74+5	12	1.74+5	6	2.60+5
B-11	9	46	1.58+5	23	1.74+5	12	1.74+5	6	2.60+5
C-12	7	50	1.06+5	37	1.06+4	19	1.06+4	10	1.06+4
N-14	11	26	1.17+6	13	1.29+6	7	1.29+6	4	1.29+6
O-16	11	50	1.06+5	25	1.17+5	13	1.17+5	7	1.17+5
Na	15	50	1.06+5	31	3.52+4	16	3.52+4	8	5.25+4
Mg	16	50	1.06+5	31	3.52+4	16	3.52+4	8	5.25+4
Al-27	11	43	2.13+5	22	2.13+5	11	2.60+5	6	2.60+5
Si	11	50	1.06+5	25	1.17+5	13	1.17+5	7	1.17+5
Ca	11	50	1.06+5	25	1.17+5	13	1.17+5	7	1.17+5
Cr	16	50	1.06+5	48	1.17+3	24	1.43+3	12	2.14+3
Mn-55	16	32	6.40+5	16	7.07+5	8	8.64+5	4	1.29+6
Fe	12	39	3.18+5	20	3.18+5	10	3.88+5	5	5.79+5
Ni	13	50	1.06+5	28	6.41+4	14	7.83+4	7	1.17+5
Zr	16	50	1.06+5	31	3.52+4	16	3.52+4	8	5.25+4
Mo	15	50	1.06+5	25	1.17+5	13	1.17+5	7	1.17+5
Pb	15	41	2.60+5	21	2.60+5	11	2.60+5	6	2.60+5
U-235	16	43	2.13+5	22	2.13+5	11	2.60+5	6	2.60+5
U-238	16	50	1.06+5	35	1.58+4	18	1.58+4	9	2.36+4

*) maximum number of terms of Legendre polynomials.

***) the energy group and the corresponding energy above which the anisotropy of elastic scattering is taken into account.

1) 1.42+7 reads 1.42×10^7 .

Table 4 Secondary gamma-ray energy structure

No.	E (MeV)	No.	E (MeV)	No.	E (MeV)
1	13.0	11	1.0	21	0.075
2	10.0	12	0.5	22	0.068
3	8.0	13	0.34	23	0.062
4	7.0	14	0.24	24	0.058
5	6.0	15	0.18	25	0.052
6	5.0	16	0.15		
7	4.0	17	0.125		
8	3.0	18	0.108		
9	2.0	19	0.094		
10	1.5	20	0.083		

Table 5 PALLAS-2DCY-FX file requirements

Logical unit	Contents	Remarks
2	Scrach	For working.
3	Calculated data for RS, ZS, PSYS	Data for RS, ZS, PSYS are calculated in Subroutine MISIMA and used in KYOTO.
5	Input	
6	Output	
8	Scrach	For working
10	Angular fluxes FN	FN for each energy mesh are stored temporarily in this unit. Large storage is necessary, for instance (75×75×28).
11	Top boundary fluxes, BOUN	Data are stored in Sub. TOKYO and used in main.
12	Calculated data for CIA	Inelastic scattering matrices CIA are calculated in Sub. YOKHAM and used in NAGOYA.
14	Reaction rates or dose rates	Data are stored in Sub. OSAKA.
15	Uncollided angular fluxes	
17	Cylindrical surface boundary fluxes, BOUNR	Data are stored in Sub. TOKYO and used in MAIN.
18	Bottom boundary fluxes, BNMZ	Data are stored in Sub. TOKYO and used in MAIN.
19	Scalar fluxes	Data are stored in Sub. OSAKA.
20	Angular fluxes calculated previously	This file is used only when input ITP20>0 (data note 11).
21	Calculated angular fluxes for all groups	This file is used only when input ITP21=1.
22	Angular fluxes calculated previously	This file is used when NBND=10 and LTAP=22.
24	Reaction rates	When ITP24>0.
25	Boundary fluxes	When NBND=10 and LTAP=25.
29	Scalar fluxes	When ITP29>0.
31	PALLAS gamma-ray library	
35	Boundary fluxes	When IRZZR>0.
51	PALLAS neutron library	for 0.1-lethargy structure.
52	PALLAS neutron library	for 0.2-lethargy structure.
54	PALLAS neutron library	for 0.4-lethargy structure.
55	PALLAS neutron library	for 0.05-lethargy structure.
58	PALLAS neutron library	for 0.8-lethargy structure.

Table 6 Relation of program variables to program mnemonics

Program mnemonic	Program variable and remark
WP (IP)	ω_p
WWP (IP)	$\Delta\omega_p$; weight for ω_p
WBP (IP)	Boundary value of $\Delta\omega_p$
WPQ (IPQ)	$\Delta\Omega_{pq}$; weight for angular mesh point
PSY (IP, IPQ)	ϕ_{pq}
PSYB (IP, IPQ)	Boundary value of ϕ_{pq}
AMU (M)	μ_m
WAMU (M)	$\Delta\mu_m$; weight for μ_m
DR (I)	Δr ; radial interval in I-th region
DZ (I)	Δz ; axial interval in I-th region
CRT (N ₁ , N ₂ , J)	$\Sigma_t(r, z, E_j)$; macroscopic total cross section in N ₁ -z and N ₂ -r region
RD (M)	r_m ; radial distance (cm)
FN (MR, MZ, IPQ)	$I(r_i, z_k, \Omega_{pq})$
SN (MR, MZ, IPQ)	$Q'(r_i, z_k, \Omega_{pq})$
ALPH (M)	α_m
ALHY (M)	α_m for hydrogen
FGM (M, J)	$\Sigma_{el}(r, E_j)f(E_j, \mu_m)$
KMAX (M)	Maximum E_k
KK (M, NONH)	$E_k(\mu_m)$ for nuclide number NONH
SIGMA (J, NUC)	$\Sigma_{el}(r, E_j)$
WT (N, IP, J)	$w_n = \phi(\omega_n^u, \omega_p, \alpha_m) - \phi(\omega_n^l, \omega_p, \alpha_m) $
GZI (N, IP, J)	$\cos^{-1} \left(\frac{\alpha_m - \omega_p \omega_n}{\sqrt{(1 - \omega_p^2)(1 - \omega_n^2)}} \right)$
RO (NUC)	$\rho = 1/A$
RS (M, IP, IPQ)	$\bar{r}_{i-1} = r'$
ZS (M, IP, IPQ)	$\bar{r}_{i-1} = z'$
PSYS (M, IP, IPQ)	$\Omega = \Omega(\omega_p, \phi)$
A (N ₁ , N ₂)	$A(\bar{r}, E)$
ION >0	(±r, +z) direction
<0	(±r, -z) direction
MUON >0	(-r, ±z) direction
<0	(+r, ±z) direction
MRR	Total number of r meshes
MZZ	Total number of z meshes
CIA (JMK, NONH)	$\frac{\Sigma_{in}(\bar{r}, E_k \rightarrow E_j) \cdot \Delta U}{4\pi}$
GZAI (NUC)	ξ
WAVE (J)	λ_j
DWAVE (J)	$\Delta\lambda_j$
GMU	$\mu = 1 + \lambda' - \lambda$
ZD (K)	Z_k ; axial distance (cm)
ORGN	$(ZZR1 + ZZR2)/2$
MRB (N ₂)	Boundary mesh numbers in N ₂ -r region
MZB (N ₁)	Boundary mesh numbers in N ₁ -z region
RB (N ₂)	Radial boundary distance
ZB (N ₁)	Axial boundary distance
EDN (N ₁ , N ₂)	$n(\bar{r})$; electron density in (N ₁ -z, N ₂ -r) region
IQT	Total angular meshes

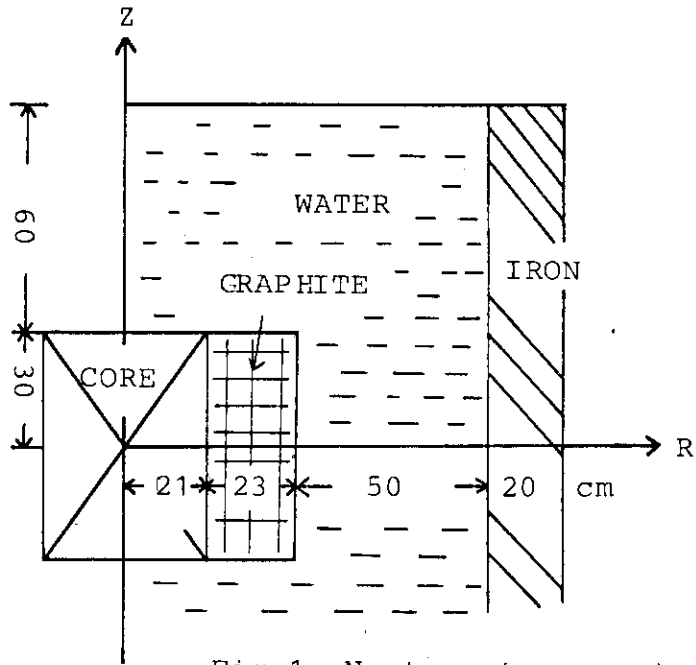


Fig.1 Neutron transport problem

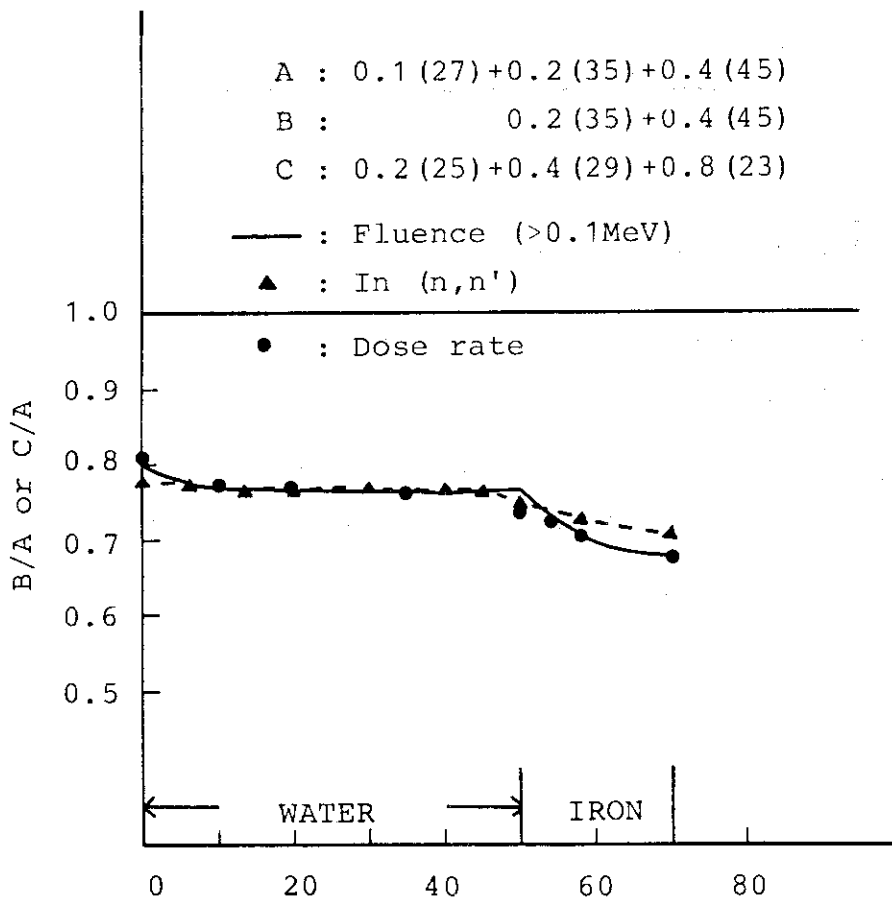


Fig.3 Accuracy of the series calculations

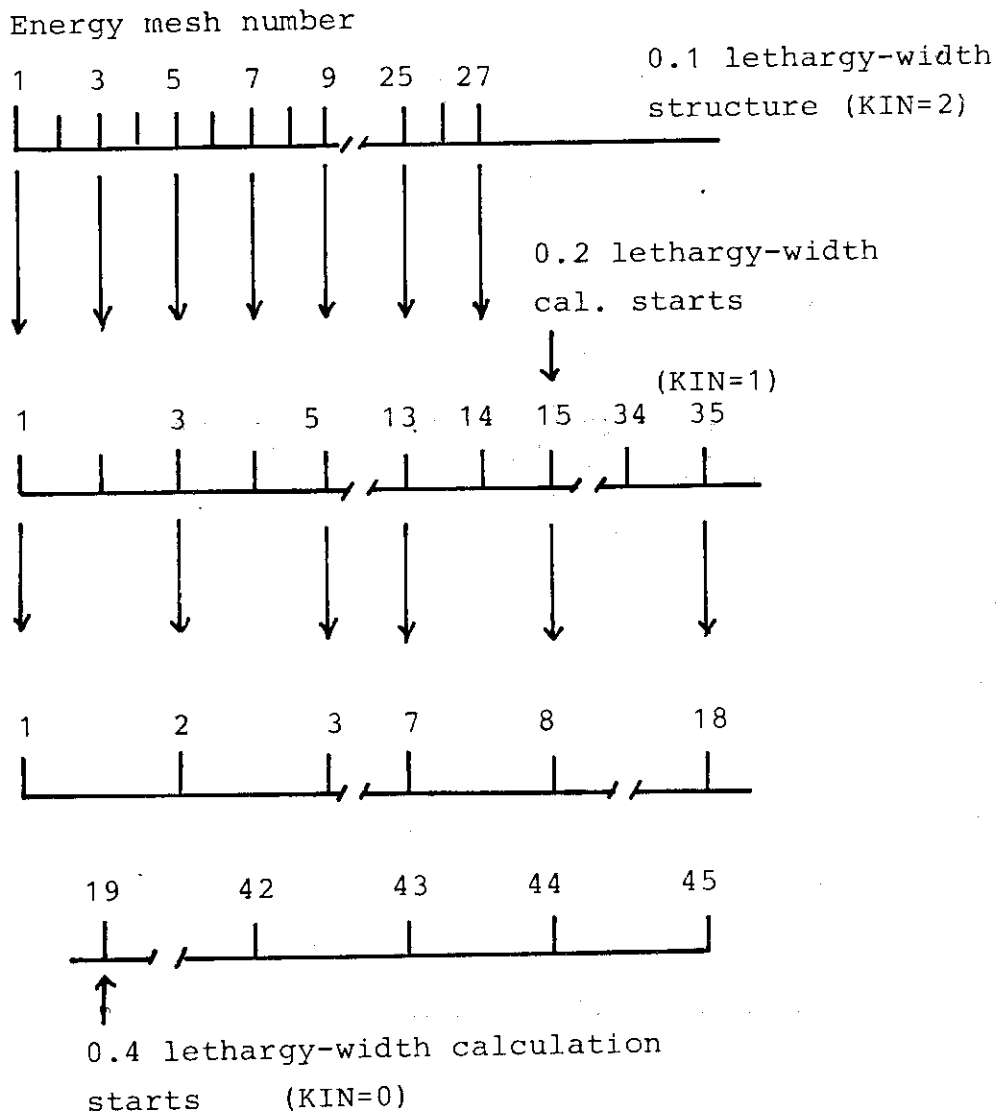


Fig.2 An example of a series calculation with 0.1(27 meshes)+0.2(35 meshes)+0.4(45 meshes) structure

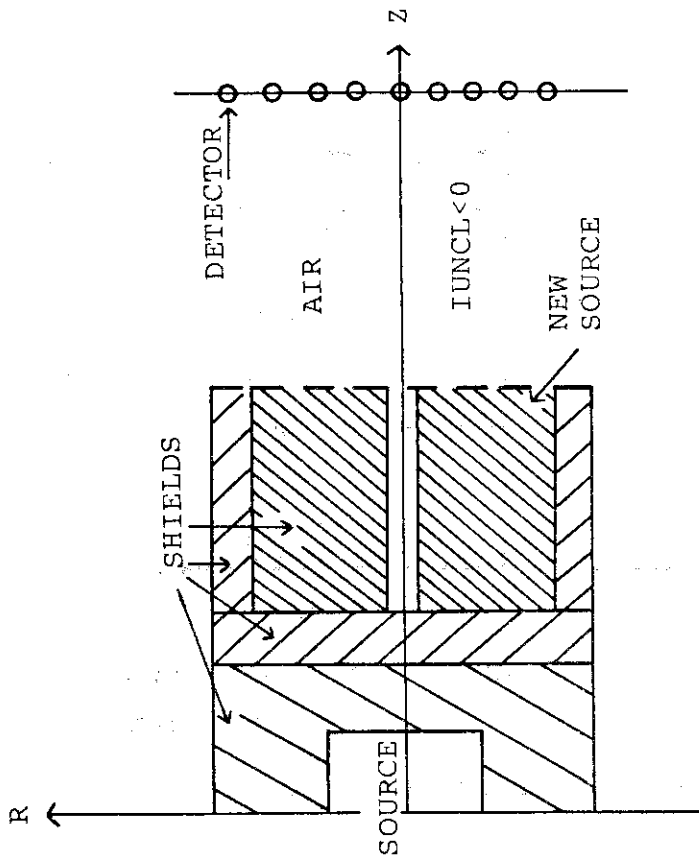


Fig.4 For IUNCL=-n, after the transport calculation based on the analytical unscattered flux calculation for a source at each energy mesh, again the analytical unscattered flux calculation is made in the air space behind the shields for the specified new source.

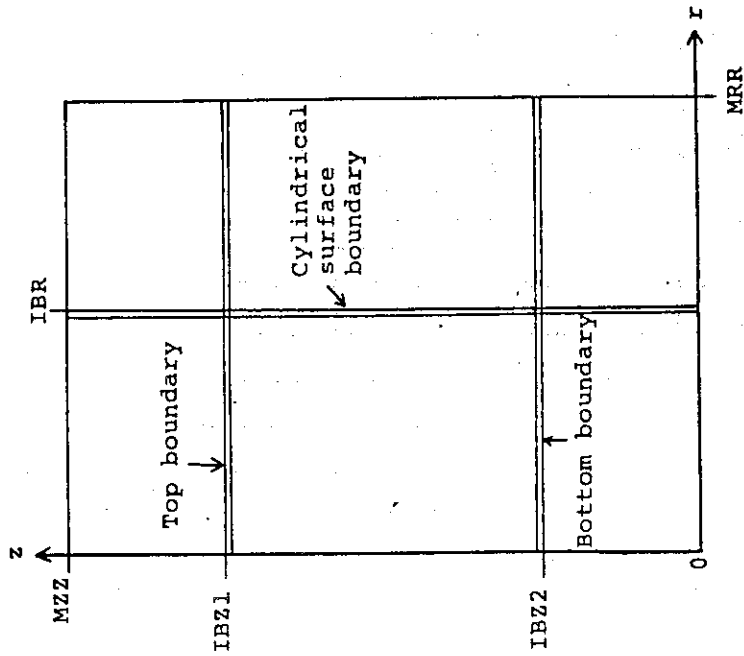


Fig. 5 Top, bottom and cylindrical surface boundary fluxes problem

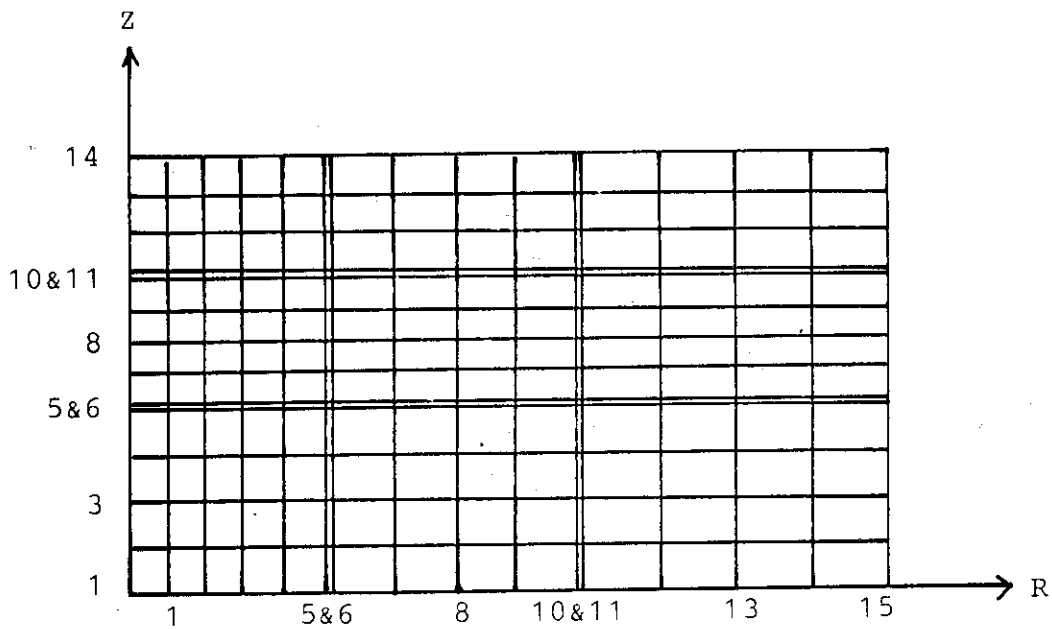


Fig.6 Spatial mesh assignment

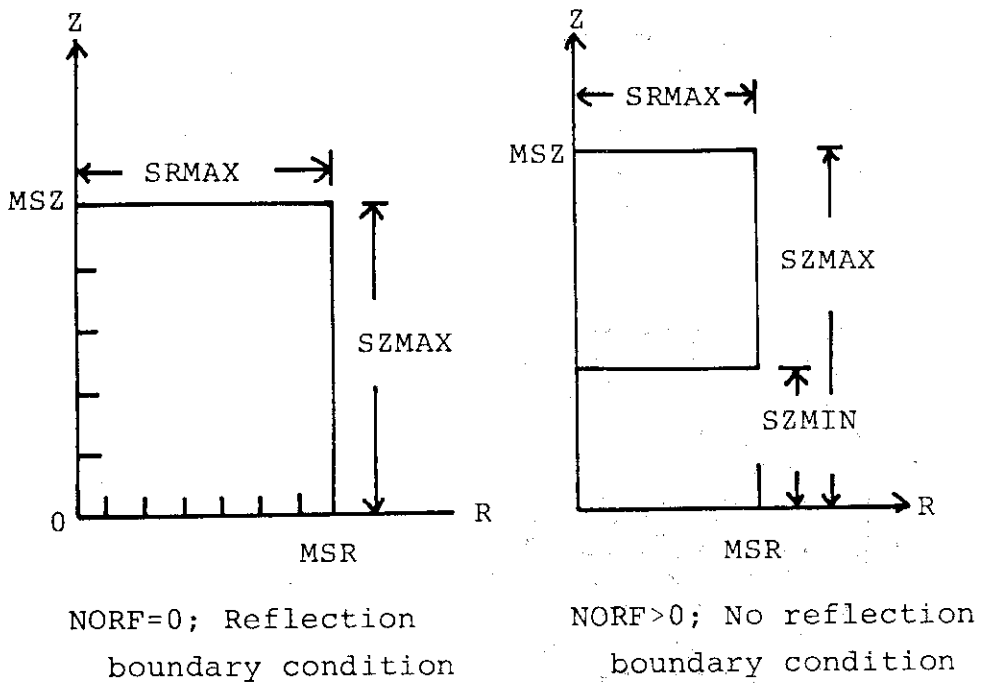


Fig.7 Cylindrical volume source specification

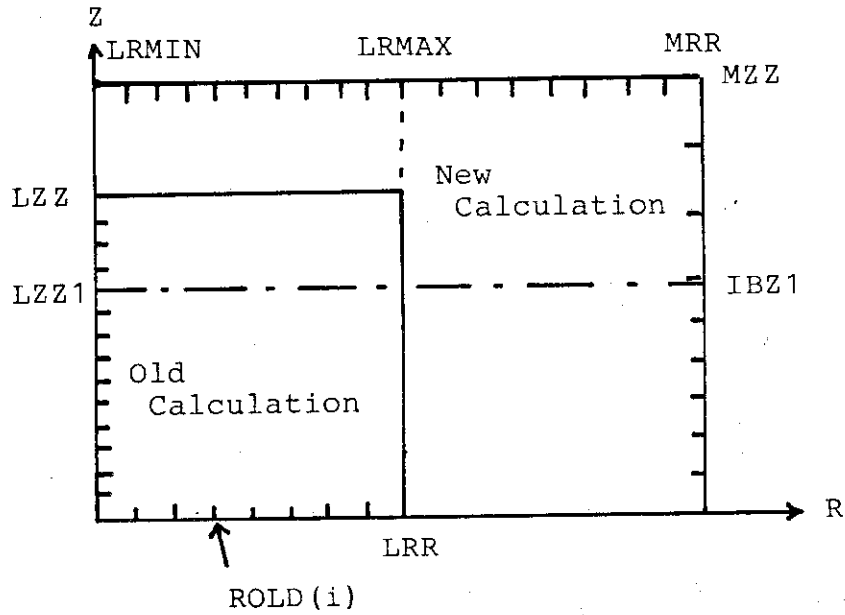


Fig.8 A new calculation with the top boundary fluxes at IBZ1-th z mesh, which are old calculations at LZZ1-th z mesh

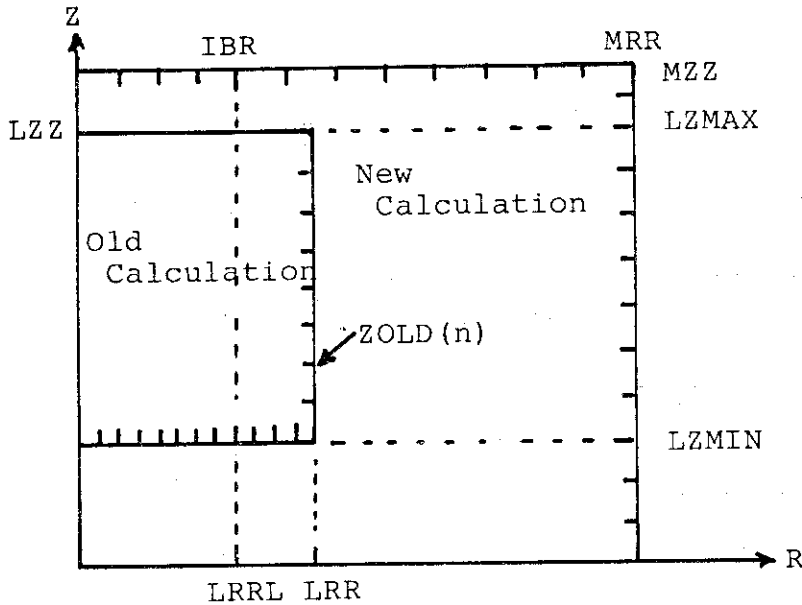


Fig.9 A new calculation with the cylindrical surface fluxes at IBR-th r mesh in old calculations at LRRL-th r mesh

STENLESS CONCR. 31	STENLESS CONCR. 22	STENLESS AIR 31 21	IRON 4
AIR 21	CONCRETE 22	AIR 21 21	IRON 4
WATER 3	REF. 2	IRON 4 LEAD 14	IRON 4
CORE 1	REF. 2	WATER 3 IRON 4	WATER 3

Fig.10 An example of identification numbers, NEK(N1,N2), of material regions

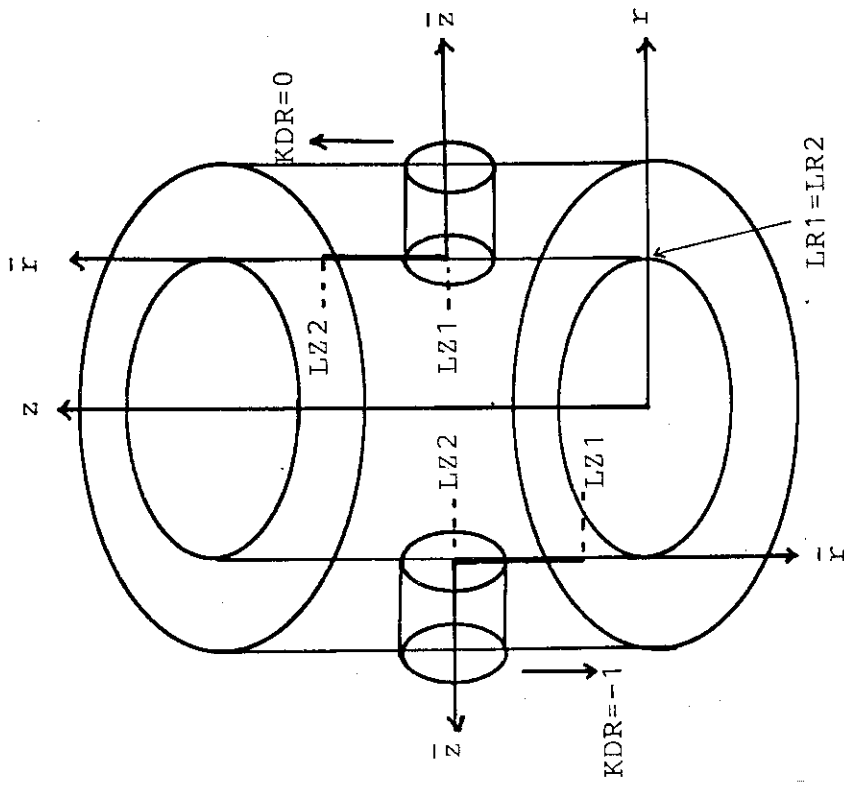


Fig.12 Conversion of angular fluxes between LZ1 and LZ2 at LR1 in (r, z) geometry to boundary angular fluxes in (\bar{r}, \bar{z}) geometry

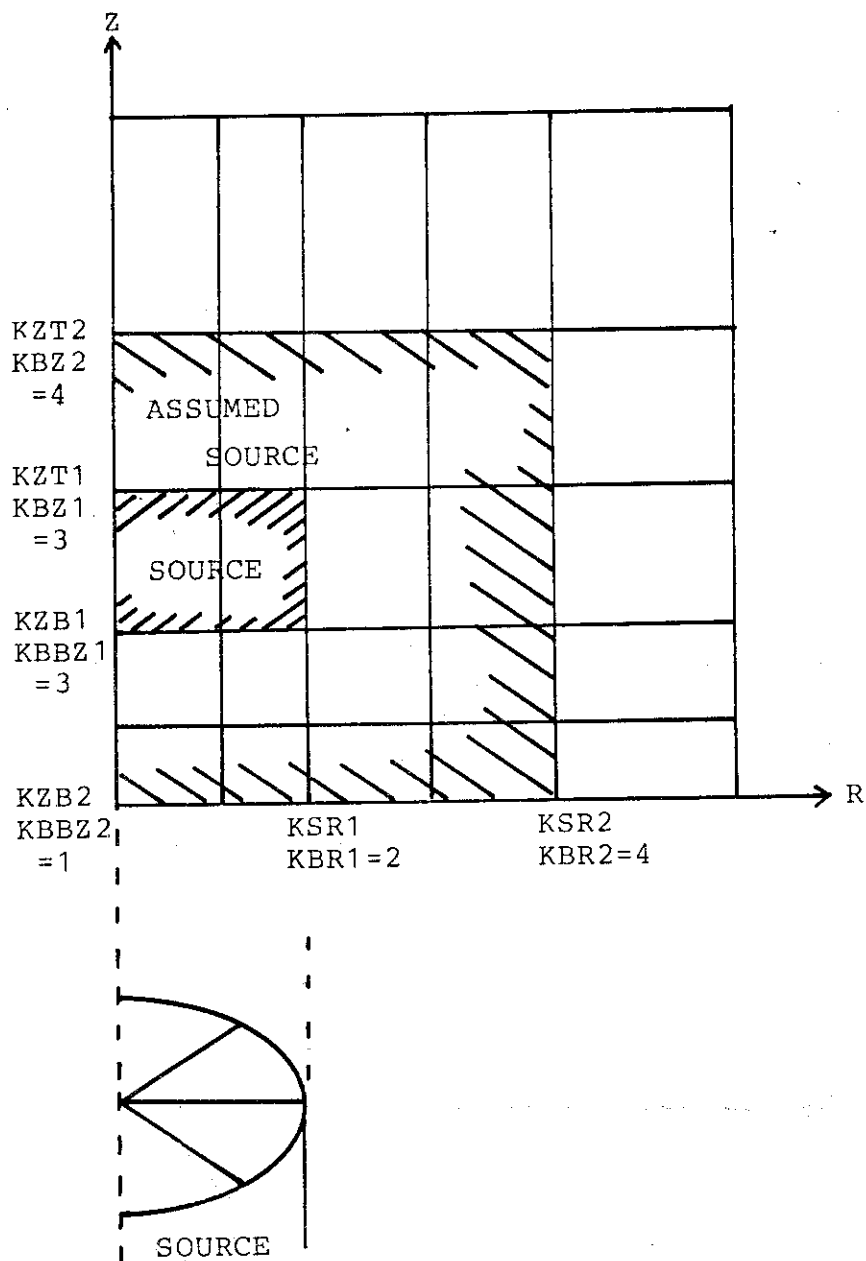


Fig.11 Source and assumed source definition in the analytical unscattered flux calculation

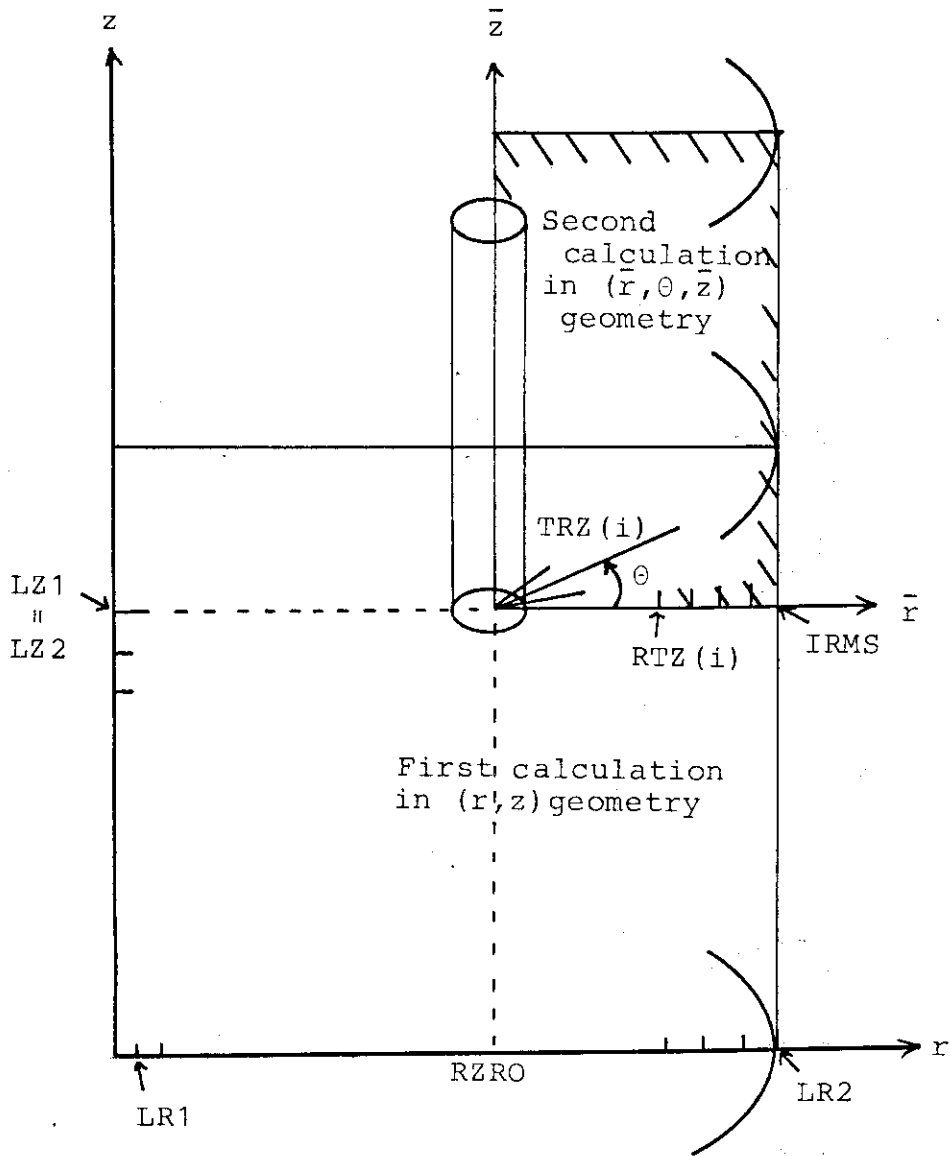


Fig.13 When $IRTZ > 0$, angular fluxes calculated in (r, z) geometry picked up between $LR1$ - and $LR2$ -radial mesh at $LZ1$ - z mesh and are converted to the boundary angular fluxes for the next calculation in $(\bar{r}, \theta, \bar{z})$ geometry.

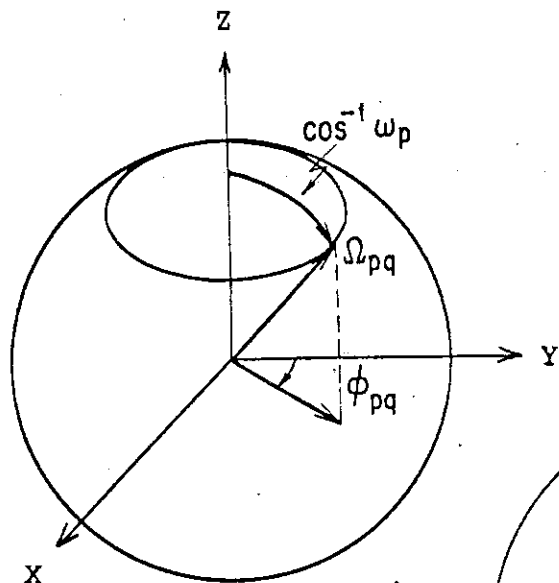


Fig.14 Discrete ordinates representation of radiation flight direction

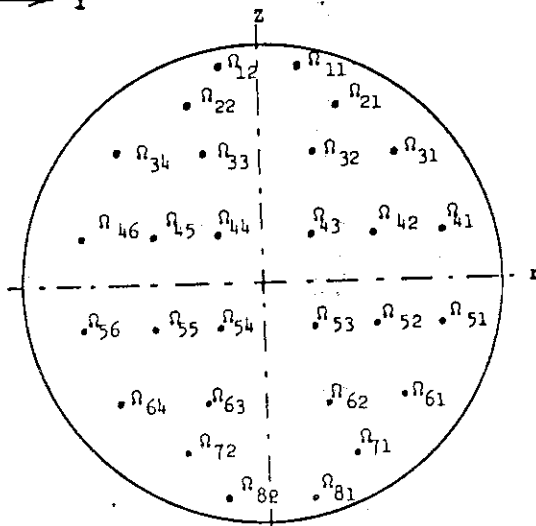


Fig.15 Angular mesh points and their order in the current PALLAS code.

Ω_{pq} and weight

p	q	ω	Weight	ϕ	Weight for Ω_{pq}
1	1	0.99240	0.015190	0.7854	0.023860
1	2	0.99240	0.015190	2.3562	0.023860
2	1	0.91174	0.14614	0.7854	0.229557
2	2	0.91174	0.14614	2.3562	0.229557
3	1	0.63852	0.40030	0.31416	0.2515165
3	2	0.63852	0.40030	1.09956	0.377275
3	3	0.63852	0.40030	2.04204	0.377275
3	4	0.63852	0.40030	2.82744	0.2515165
4	1	0.219185	0.43837	0.19635	0.172148
4	2	0.219185	0.43837	0.687225	0.258222
4	3	0.219185	0.43837	1.27630	0.258222
4	4	0.219185	0.43837	1.86533	0.258222
4	5	0.219185	0.43837	2.4544	0.258222
4	6	0.219185	0.43837	2.9453	0.172148

```

*****
* INPUT DATA LIST *
*****
1.....2.....3.....4.....5.....6.....7.....8
SAMPLE PROBLEM 1 FEHQ JRR-4 IRON - WATER 2D(R,Z)
1 2 0 0 0 0 0
27 4 2 0 1 51 0 0
0 0 0 0 0 0 0
14.20 0.10 7.657E 10
6 6 16 6 21.06 23.20 50.0 20.0
11 11 30.0 60.0
6 11 0 21.06 30.00
1.100 1.037 0.9473 0.718 0.5485
1.510 1.500 1.450 1.250 1.100 0.885
0.780 0.710 0.67
0 0
0.0 3 1 2 1
17 3 1 2 1
2 2 2 1
19 1 2 3 4
3 3 3 4
CORE
HY
1011 4.577E-02
OXY
1086 2.291E-02
AL
1137 1.842E-02
REF
C
1062 7.441E-02
WATER
HY
1011 0.06674
OXY
1086 0.03337
IRON
FE
1260 8.470E-02
0 0
0 0 3 0 0 21 34 1 7
INT FLUX(0.1MEV)
1.000 1.000 1.000 1.000 1.000 1.000 1.000 1.000 1.000 1.000
1.000 1.000 1.000 1.000 1.000 1.000 1.000 1.000 1.000 1.000
1.000 1.000 1.000 1.000 1.000 1.000 1.000 1.000 1.000 1.000
IN(N,N') 0.1 LETH
6.627E-02 1.028E-01 0.1654 0.2242 0.2886 0.2959 0.3071
0.3350 0.3368 0.3260 0.3146 0.3217 0.3305 0.3319
0.5355 0.3327 0.3171 0.2844 0.2380 0.2035 0.1841 0.1533
0.1259 0.1012 7.605E-02 5.708E-02 4.006E-02 2.541E-02 1.703E-02 1.014E-02
.....1.....2.....3.....4.....5.....6.....7.....8

```

Fig.16-1 Input data for Sample problem 1

101	6.627E-02	0.1654	0.2631	0.2959	0.3350	0.3260	0.3112	0.3305
102	0.3355	0.3171	0.2380	0.1841	0.1259	7.605E-02	4.006E-02	1.703E-02
103	4.836E-03	2.348E-03	1.138E-03	1.100E-04	0.0			
104	0.0							
105	0.0							
106	45	4	2	0	1	54		
107	0	0	0	0	0	0		
108	14.20	0.40	7.657E 10					
109	6	6	16	6				
110	21.06	23.20	50.0	20.0				
111	11	11						
112	30.0	60.0						
113	6	11	0					
114	0.0	21.06	0.0	30.00				
115	1.100	1.037	0.9473	0.8476	0.718	0.5485		
116	1.510	1.500	1.450	1.360	1.250	1.120	1.100	0.885
117	0.780	0.710	0.67					
118	10120							
119	0.01							
120	3	1	2	1				
121	2	2	1					
122	1	2	3	4				
123	3	3	3	4				
124	CORE							
125	HY							
126	4011	4.577E-02						
127	OXY							
128	4086	2.291E-02						
129	AL							
130	4137	1.842E-02						
131	REF							
132	C							
133	4062	7.441E-02						
134	WATER							
135	HY							
136	4011	0.06674						
137	OXY							
138	4086	0.03337						
139	IRON							
140	FE							
141	4260	8.470E-02						
142	0	0	0	0	21	34	1	7
143	0	0	0	0	0	0	0	0

*** INPUT DATA END *** Fig.16-3 (Continued)

```

*** INPUT DATA
SAMPLE PROBLEM 1 FEHO JRR-4 IRON - WATER 2D(R,Z)
***
KNDG,KIN,NORF,KYST,MONOE, MNODRE,IPRNT,IRZZR,IRTZ = 1 2 0 0 0 0 0 0 0 0
INPUT DATA NO.1
E-MAX = 1.420E+01 ENERGY MESH = 27 LETHARGY WIDTH= 1.000E-01
SOURCE NORMALIZATION = 7.6570E+10 NNI( LIB.DISK NO.) = 51
UNCOLLIDED FLUX CAL. OPTION = 0 FISSION SOURCE = 1 START ENERGY MESH = 1
REGION 1 2 3 4 5 6 7 8 9 10
R-MESHES = 6 6 16 6
R-THICKNESS= 2.106E+01 2.320E+01 5.000E+01 2.000E+01
Z-MESHES = 11 11
Z-THICKNESS= 3.000E+01 6.000E+01
NBND,IBZ1,IBZ2,IBR,LTAP,JOAK,IRWTR = 0 0 0 0 0 0 0 0 0 0
ENERGY POINTS(MEV)
E(J)(MEV) = 1.4200E+01 1.2849E+01 1.1626E+01 1.0520E+01 9.5185E+00 8.6127E+00 7.7931E+00 7.0515E+00 6.3805E+00 5.7733E+00
E(J)(MEV) = 5.2239E+00 4.7268E+00 4.2770E+00 3.8700E+00 3.5017E+00 3.1684E+00 2.8669E+00 2.5941E+00 2.3472E+00 2.1239E+00
E(J)(MEV) = 1.9218E+00 1.7389E+00 1.5734E+00 1.4237E+00 1.2882E+00 1.1656E+00 1.0547E+00
ANGULAR QUADRATURE AND WEIGHT
WP(IP) = 0.992400 0.911740 0.638520 0.219185 -0.219185 -0.638520 -0.911740 -0.992400
WPP(IP)= 0.015190 0.146140 0.400300 0.438370 0.438370 0.400300 0.146140 0.015190
WPG(IP)= 0.023860 0.023860 0.229557 0.229557 0.229557 0.229557 0.229557 0.229557 0.251517 0.251517
WQ(IP)= 0.258222 0.258222 0.258222 0.172148 0.172148 0.258222 0.258222 0.258222 0.258222 0.172148
WR(IP)= 0.251517 0.377275 0.377275 0.229557 0.229557 0.229557 0.229557 0.229557 0.023860 0.023860
PSY(P,PQ)= 0.785400 0.785400 0.314160 0.198350 0.356200 1.099360 0.687225
PSY(P,PQ)= 0.0 0.0 2.042040 1.276300 0.0 0.0 2.827440 1.865330
PSY(P,PQ)= 0.0 0.0 0.0 2.454400 0.0 0.0 0.0 2.945300
PSYB(P,PQ)= 1.570800 1.570800 0.628320 0.392700 0.0 0.0 1.570800 0.981750
PSYB(P,PQ)= 0.0 0.0 2.513280 1.570800 0.0 0.0 0.0 0.0
PSYB(P,PQ)= 0.0 0.0 0.0 2.748900
SPATIAL MESH ASSIGNMENT
RADIUS(CM)= 3.5100E+00 7.0200E+00 1.0530E+01 1.4040E+01 1.7550E+01 2.1060E+01 2.4600E+01 2.8160E+01 3.1740E+01 3.5340E+01
RADIUS(CM)= 3.9620E+01 4.4260E+01 4.8900E+01 5.3540E+01 5.8180E+01 6.2820E+01 6.7460E+01 7.2100E+01 7.6740E+01 8.1380E+01
RADIUS(CM)= 7.0927E+01 7.4260E+01 7.7593E+01 8.0927E+01 8.4260E+01 8.7593E+01 9.0927E+01 9.4260E+01 9.7593E+01 1.00927E+02
RADIUS(CM)= 1.0226E+02 1.0626E+02 1.1026E+02 1.1426E+02
Z-MESH(CM)= 0.0 3.0000E+00 6.0000E+00 9.0000E+00 1.2000E+01 1.5000E+01 1.8000E+01 2.1000E+01 2.4000E+01 2.7000E+01
Z-MESH(CM)= 3.0000E+01 3.0000E+01 3.6000E+01 4.2000E+01 4.8000E+01 5.4000E+01 6.0000E+01 6.6000E+01 7.2000E+01 7.8000E+01
Z-MESH(CM)= 8.4000E+01 9.0000E+01
MSR MSZ IVS = 6 11 0
SRMIN SRMAX SZMIN SZMAX = 0.0 2.106E+01 0.0 3.000E+01
TOTAL SOURCE, NORM.FACTOR = 7.7191E+04 9.9195E+05
SOURCE
MSR,MSZ,IVS,RZR,ZZR1,ZZR2 = 6 11 0 2.1060E+01 3.0000E+01 0.0
SR(N) = 1.0911E+06 1.0287E+06 9.3967E+05 8.4078E+05 7.1222E+05 5.4408E+05
SZ(N) = 1.5100E+00 1.5000E+00 1.4500E+00 1.3600E+00 1.2500E+00 1.1200E+00 1.0000E+00 8.8500E-01 7.8000E-01 7.1000E-01
SE(N) = 3.3982E-05 1.0121E-04 2.6845E-04 6.4151E-04 1.3957E-03 2.7908E-03 5.1726E-03 8.9556E-03 1.4584E-02 2.2478E-02
SE(N) = 3.2976E-02 4.6279E-02 6.2435E-02 8.1224E-02 1.0237E-01 1.2537E-01 1.4964E-01 1.7452E-01 1.9937E-01 2.2357E-01
SE(N) = 2.4657E-01 2.6791E-01 2.8722E-01 3.0423E-01 3.1883E-01 3.3090E-01 3.4046E-01
LTHAL,LCUT,EPSRN = 0 0 0.0

```

Fig.16-4 List of input data for sample problem 1

NUMBER OF ELEMENT IN EACH REGION
 NOEL = 3 1 2 1
 NOEL = 2 2 2 1
 MATERIAL NUMBER OF EACH REGION
 NEK = 1 2 3 4
 NEK = 3 3 3 4

TOTAL R-MESH = 34 TOTAL Z-MESH = 22
 JSAT,J11,J12,JJ,NNI(READ(NNI) DATA) = 1 1 27 27 51

*** NUCLEAR DATA **

MATERIAL = CORE
 NNI IN READ = 51
 MAXG,NGG,JAM,JBM,JFMU,LP,JPM= 50 25 50 1 0 1 50

NUCLIDE = H1 JULY,1981 (PROCESSED WITH NJOY AT JAERI)

MATNO = 1011
 MAXG/JFMU/LL = 50 0 1
 PL-ORDER(IF 0 MEANS MAX) PL-TERMS(L1,L2)= 0 1 1
 AMAS = 1.000 ATOMIC DENSITY = 0.4577E-01
 SIGMA-T = 0.6898 0.7578 0.8305 0.9085 0.9908
 SIGMA-T = 1.588 1.705 1.826 1.952 2.083
 SIGMA-T = 2.985 3.159 3.341 3.530 3.726
 SIG-C = 0.2970E-04 0.3044E-04 0.3142E-04 0.3225E-04 0.3299E-04 0.3360E-04 0.3428E-04 0.3515E-04 0.3588E-04 0.3594E-04
 SIG-C = 0.3628E-04 0.3638E-04 0.3630E-04 0.3618E-04 0.3597E-04 0.3578E-04 0.3548E-04 0.3509E-04 0.3473E-04 0.3441E-04
 SIG-C = 0.3425E-04 0.3428E-04 0.3432E-04 0.3436E-04 0.3446E-04 0.3442E-04 0.3445E-04
 SIGMA-S = 0.6898 0.7578 0.8304 0.9085 0.9908 1.077 1.170 1.267 1.368 1.476
 SIGMA-S = 1.588 1.705 1.826 1.952 2.083 2.220 2.361 2.507 2.660 2.820
 SIGMA-S = 2.985 3.159 3.341 3.530 3.726 3.930 4.145 4.361 4.600 4.820
 NNI IN READ = 51
 MAXG,NGG,JAM,JBM,JFMU,LP,JPM= 50 25 50 9 50 10 50

NUCLIDE = 016 JULY,1981 (PROCESSED WITH NJOY AT JAERI)

MATNO = 1086
 MAXG/JFMU/LL = 50 50 10
 PL-ORDER(IF 0 MEANS MAX) PL-TERMS(L1,L2)= 0 10 1
 AMAS = 16.000 ATOMIC DENSITY = 0.2291E-01
 SIGMA-T = 1.645 1.570 1.684 1.353 1.223
 SIGMA-T = 1.263 1.278 1.784 2.306 3.147
 SIGMA-T = 2.112 1.759 2.076 2.419 3.757
 SIG-C = 0.7541E-08 0.7925E-08 0.8328E-08 0.8660E-08 0.9186E-08 0.9624E-08 0.1025E-07 0.1002E-07 0.1147E-07 0.1145E-07
 SIG-C = 0.9320E-08 0.1274E-07 0.1315E-07 0.1908E-07 0.1542E-07 0.1282E-07 0.1897E-07 0.1783E-07 0.1698E-07 0.1949E-07
 SIG-C = 0.2041E-07 0.2150E-07 0.2261E-07 0.2371E-07 0.2501E-07 0.2621E-07 0.2747E-07
 SIGMA-S = 0.9788 1.020 1.133 0.9285 0.8344 0.8735 0.8638 0.9319 0.8396 1.276
 SIGMA-S = 1.181 1.206 1.694 2.282 3.144 2.066 2.066 1.087 0.8764 1.404
 SIGMA-S = 2.112 1.759 2.076 2.419 3.757 2.920 2.920 1.155 1.155 1.308
 NNI IN READ = 51
 MAXG,NGG,JAM,JBM,JFMU,LP,JPM= 50 25 50 29 50 10 50

NUCLIDE = AL27 JULY,1981 (PROCESSED WITH NJOY AT JAERI)

MATNO = 1137
 MAXG/JFMU/LL = 50 50 10
 PL-ORDER(IF 0 MEANS MAX) PL-TERMS(L1,L2)= 0 10 1
 AMAS = 27.000 ATOMIC DENSITY = 0.1842E-01
 SIGMA-T = 1.744 1.735 1.743 1.699 1.714
 SIGMA-T = 2.155 2.171 2.254 2.499 2.499 1.747 1.825 1.896 2.009 2.065
 SIGMA-T = 2.155 2.171 2.254 2.499 2.499 2.464 2.642 3.171 2.686 3.134

Fig.16-5 (Continued)

 * INPUT DATA LIST *

	1	2	3	4	5	6	7	8
1	SAMPLE PROBLEM 2 82-11 NO.2 PAL2DST.DATA(MIURA1) FLUX TO DISK							
2	4	0	10	0	0	0	0	0
3	32	7	10	17	0	0	0	
4	1	0	0	0				
5	8.250		0.0					
6	6	3	4	3	11	10	6	
7	12.50			2.750		2.750	3.000	35.4 90.30 22.6
8	2	3	3	7	6	11	4	3 10 6
9	535.0		5.0		195.0		35.0	50.0 50.0 15.0 2.5
10	142.5		30.0					
11	8.250		7.750		7.250		6.750	6.250 5.750 5.250 4.750
12	4.250		3.750		3.250		2.750	2.250 1.750 1.250 1.000
13	0.750		0.600		0.500		0.400	0.320 0.260 0.200 0.170
14	0.145		0.130		0.120		0.110	0.100 0.092 0.085 0.080
15	0	2						
16	2.050E 05	3.350E 06	1.350E 06	1.550E 06	2.050E 06	2.150E 06	3.480E 06	4.400E 06
17	7.400E 06	6.900E 06	1.000E 07	8.000E 06	1.440E 07	1.160E 07	4.900E 06	4.300E 06
18	3.600E 06	3.600E 06	4.000E 06	4.200E 06	4.300E 06	4.400E 06	4.400E 06	4.400E 06
19	4.400E 06	4.400E 06	4.400E 06	4.400E 06	4.400E 06	4.400E 06	4.400E 06	4.400E 06
20	1	1	1	1	1	1	1	1
21	1	-1	-1	-1	-1	-1	-1	-1
22	1	1	1	1	1	1	1	1
23	1	1	1	1	1	1	1	1
24	1	1	1	1	1	1	1	1
25	1	1	1	1	1	1	1	1
26	1	1	1	1	1	1	1	1
27	1	1	1	1	1	1	1	1
28	1	1	1	1	1	1	1	1
29	1	1	1	1	1	1	1	1
30	1	1	1	1	1	1	1	1
31	0	12	13	13	13	13	13	13
32	0	0	1	1	1	1	1	1
33	0	0	0	34	35	35	35	35
34	0	0	0	1	1	1	35	35
35	35	35	35	35	35	1	35	35
36	61	61	61	61	61	1	35	35
37	34	34	34	34	34	1	35	35
38	1	1	1	1	1	1	35	35
39	35	35	35	35	35	35	35	35
40	1	1	1	1	1	1	1	1
41	1	1	1	1	1	1	1	1
42	1	1	1	1	1	1	1	1
43	1	1	1	1	1	1	1	1
44	1	1	1	1	1	1	1	1
45	1	1	1	1	1	1	1	1
46	1	1	1	1	1	1	1	1
47	1	1	1	1	1	1	1	1
48	1	1	1	1	1	1	1	1
49	1	1	1	1	1	1	1	1
50	1	1	1	1	1	1	1	1

Fig.17-1 Input data for Sample problem 2

1.....2.....3.....4.....5.....6.....7.....8	
51	AIR								51
52	550								52
53	0.0	0.0	1.200E-03						53
54	ABSOR1								54
55	1.000E-04								55
56	8.900E-02	8.900E-02	8.900E-02	8.900E-02	8.900E-02	8.900E-02	8.900E-02	8.900E-02	56
57	8.900E-02	8.900E-02	8.900E-02	8.900E-02	8.900E-02	8.900E-02	8.900E-02	8.900E-02	57
58	8.900E-02	8.900E-02	8.900E-02	8.900E-02	8.900E-02	8.900E-02	8.900E-02	8.900E-02	58
59	8.900E-02	8.900E-02	8.900E-02	8.900E-02	8.900E-02	8.900E-02	8.900E-02	8.900E-02	59
60	0.000								60
61	0.000								61
62	0.000								62
63	0.000								63
64	ABSORB2								64
65	1.000E-04								65
66	4.000E-00	4.056E-00	4.008E-00	4.002E-00	4.009E-00	4.009E-00	4.008E-00	4.621E-00	66
67	4.041E-00	4.041E-00	4.049E-00	4.009E-00	4.004E-00	4.068E-00	4.067E-00	4.418E-00	67
68	4.024E-00	4.098E-00	4.045E-00	4.034E-00	4.041E-00	4.045E-00	4.025E-00	4.031E-00	68
69	4.024E-00	4.098E-00	4.045E-00	4.034E-00	4.041E-00	4.045E-00	4.025E-00	4.031E-00	69
70	0.0								70
71	0.0								71
72	0.0								72
73	0.0								73
74	LEAD								74
75	820								75
76	0.0	0.08	11.34						76
77	CONCRE								77
78	520								78
79	0.0	0.0	2.25						79
80	IRON								80
81	260								81
82	0.0	0.0	7.86						82
83	0 10								83
84	1 40 15 15								84
85	0 0 0 0 0 1 5 31 40								85

*** INPUT DATA END ***

Fig.17-2 (Continued)

ANGULAR DISTRIBUTION OF POINT SOURCE
 0.398E-01 0.398E-01 0.398E-01 0.398E-01 0.398E-01 0.398E-01 0.398E-01 0.398E-01 0.398E-01 0.398E-01
 ANGULAR DISTRIBUTION OF POINT SOURCE
 0.398E-01 0.398E-01 0.398E-01 0.398E-01 0.398E-01 0.398E-01 0.398E-01 0.398E-01 0.398E-01 0.398E-01
 ANGULAR DISTRIBUTION OF POINT SOURCE
 0.398E-01 0.398E-01 0.398E-01 0.398E-01 0.398E-01 0.398E-01 0.398E-01 0.398E-01 0.398E-01 0.398E-01
 SE(N) = 2.0500E+05 3.3500E+06 1.3500E+06 1.5500E+06 2.0500E+06 2.1500E+06 3.4800E+06 4.4000E+06 6.9000E+06
 SE(N) = 1.0000E+07 8.0000E+06 1.4400E+07 1.1600E+07 4.9000E+06 4.3000E+06 3.6000E+06 3.6000E+06 4.2000E+06
 SE(N) = 4.3000E+06 4.4000E+06 4.4000E+06 4.4000E+06 4.4000E+06 4.4000E+06 4.4000E+06 4.4000E+06 4.4000E+06
 SE(N) = 4.4000E+06 4.4000E+06

NUMBER OF ELEMENT IN EACH REGION
 NOEL = 1 1 1 1 1 1 1 1 1 1
 NOEL = 1 -1 -1 -1 -1 -1 -1 -1 -1 -1
 NOEL = 1 1 1 1 1 1 1 1 1 1
 NOEL = 1 1 1 1 1 1 1 1 1 1
 NOEL = 1 1 1 1 1 1 1 1 1 1
 NOEL = 1 1 1 1 1 1 1 1 1 1
 NOEL = 1 1 1 1 1 1 1 1 1 1
 NOEL = 1 1 1 1 1 1 1 1 1 1

MATERIAL NUMBER OF EACH REGION
 NEK = 1 1 1 1 1 1 1 1 1 1
 NEK = 0 12 13 13 13 13 13 13 13 13
 NEK = 0 0 1 1 1 1 1 1 1 1
 NEK = 0 0 0 34 35 35 35 35 35 35
 NEK = 0 0 0 1 1 1 1 1 1 1
 NEK = 35 35 35 35 35 35 35 35 35 35
 NEK = 61 61 61 61 61 61 61 61 61 61
 NEK = 34 34 34 34 34 34 34 34 34 34
 NEK = 1 1 1 1 1 1 1 1 1 1
 NEK = 35 35 35 35 35 35 35 35 35 35

INDICATOR OF SOURCE POSITION IN UNCLFX
 KSR1, KBR1, KZT1, KBZ1, KBZ1, KBBZ1, NPHI = 1 1 1 1 1 1 1 1 1 1

INDICATOR OF UNCL. CAL. UNCOLLIDED FLUXES
 IUNC = 1 1 1 1 1 1 1 1 1 1
 IUNC = 1 1 1 1 1 1 1 1 1 1
 IUNC = 1 1 1 1 1 1 1 1 1 1
 IUNC = 1 1 1 1 1 1 1 1 1 1
 IUNC = 1 1 1 1 1 1 1 1 1 1
 IUNC = 1 1 1 1 1 1 1 1 1 1
 IUNC = 1 1 1 1 1 1 1 1 1 1
 IUNC = 1 1 1 1 1 1 1 1 1 1

KSR2, KBR2, KZT2, KBZ2, KZB2, KBBZ2 = 0 0 0 0 0 0 0 0 0 0
 IUNB = 0 0 0 0 0 0 0 0 0 0
 IUNB = 0 0 0 0 0 0 0 0 0 0
 IUNB = 0 0 0 0 0 0 0 0 0 0
 IUNB = 0 0 0 0 0 0 0 0 0 0
 IUNB = 0 0 0 0 0 0 0 0 0 0
 IUNB = 0 0 0 0 0 0 0 0 0 0
 IUNB = 0 0 0 0 0 0 0 0 0 0

Fig.17-4 (Continued)


```

*****
*                               *
*   INPUT DATA LIST   *
*                               *
*****

.....1.....2.....3.....4.....5.....6.....7.....8
1  SAMPLE PROBLEM 3 PL2DRZ.DATA(CS137) WATER POOL FOR SPENT FUEL 59-11- 6
2  4 0 0 0 10
3  31 2 2 0 0
4  0 0 0
5  0.662      0.04      0.0
6  30 5
7  2000.0     40.0
8  11 19
9  200.0      435.0
10 30 11
11 0.0        1000.0    0.000    300.0    629.0    629.0    629.0    629.0
12 629.0      629.0     629.0    629.0    629.0    629.0    629.0    629.0
13 629.0      629.0     629.0    629.0    629.0    629.0    629.0    629.0
14 629.0      629.0     629.0    629.0    629.0    629.0    629.0    629.0
15 629.0      629.0     629.0    629.0    629.0    629.0    629.0    629.0
16 1.000      1.000     1.000    1.000    1.00    1.000    1.000    1.000
17 1.000      1.000     1.000
18 1.000
19 1 1
20 1 1
21 1 1
22 11 11
23 WATER
24 540
25 0.0        0.0        1.00
26 AIR
27 550
28 0.0        0.0        1.200E-03
29 0 10
30 1 30 30 30
31 0 0 0 0 1 1 10 11 30
.....1.....2.....3.....4.....5.....6.....7.....8

*** INPUT DATA END ***

```

Fig.18 Input data for Sample problem 3

 * INPUT DATA LIST *

```

.....*.....1.....*.....2.....*.....3.....*.....4.....*.....5.....*.....6.....*.....7.....*.....8
1  SAMPLE PROBLEM 4 PL2DRZ.DATA(CSSKY) GAMMA-RAY SKYSHINE CS-137 POOL
2  4 0 10 0 0 0 0 0
3  31 4 4 25 0 0 0 0
4  10 6 0 0 22 2 0
5  0.662 0.04
6  10 6 11 26
7  2000.0 50.00 10000.0 100000.0
8  5 5 6 21
9  32.0 1000.0 2500.0 60000.0
10 30 1 1 0 1 10 1 10
11 66.66 133.33 200.0 266.66 333.33 400.0 466.66 533.33
12 600.0 666.66 733.33 800.00 866.66 933.33 1000.0 1066.66
13 1133.33 1200.00 1266.66 1333.33 1400.0 1466.66 1533.33 1600.0
14 1666.66 1733.33 1800.00 1866.66 1933.33 2000.0
15 -1 -1 1 1
16 1 -1 1 1
17 1 1 1 1
18 1 1 1 1
19 1 1 3 3
20 11 1 11 11
21 11 11 11 11
22 11 11 11 11
23 10 1 6 1 1 1 4
24 0 0 0 0
25 0 0 1 1
26 1 1 1 1
27 1 1 1 1
28 ABS
29 0.0001
30 1.000 1.000 1.000 1.000 1.000 1.000 1.000 1.00
31 1.000 1.000 1.000 1.000 1.000 1.000 1.000 1.00
32 1.000 1.000 1.000 1.000 1.000 1.000 1.000 1.00
33 1.000 1.000 1.000 1.000 1.000 1.000 1.000 1.00
34 0.00
35 0.00
36 0.00
37 0.00
38 SOIL
39 520
40 0. 0.0 1.50
41 AIR
42 550
43 0. 0.0 1.200E-03
44 0 0
45 0 0 0 0 1 17 35 6 15
.....*.....1.....*.....2.....*.....3.....*.....4.....*.....5.....*.....6.....*.....7.....*.....8
*** INPUT DATA END ***
  
```

Fig.19-1 Input data for Sample problem 4


```

*** SAMPLE PROBLEM 4 PL2DR1.DAT(CSSKY) GAMMA-RAY SKYSHINE CS-137 POOL ***
INPUT DATA
KNGG.KIN.NORF.KTST.MONOE, MNODRE,IPRNT,IRZRR,IRTZ = 4 0 10 0 0 0 0 0 0 0
INPUT DATA NO.1
E-MAX = 6.620E-01 ENERGY MESH = 31 LEHARGY WIDTH= 4.000E-02
SOURCE NORMALIZATION = 0.0 NNI(LIB.DISK NO.) = 0
UNCOLLIDED FLUX CAL. OPTION = 25 FISSION SRCE = 0 START ENERGY MESH = 1
REGION 1 2 3 4 5 6 7 8 9 10
R-MESHES = 10 6 11 26
R-THICKNESS = 2.000E+03 5.000E+01 1.000E+04 1.000E+05
Z-MESHES = 5 5 6 21
Z-THICKNESS = 3.200E+01 1.000E+03 2.500E+03 6.000E+04
NBND,IBZ1,IBZ2,IBR,LTAP,JOAK,IRVTR = 10 6 0 0 22 2 0
ENERGY POINTS(MEV)
E(J)(MEV) = 6.6200E-01 6.2200E-01 5.7995E-01 5.3643E-01 4.9212E-01 4.4773E-01 4.0401E-01 3.6163E-01 3.2120E-01 2.8320E-01
E(J)(MEV) = 2.4800E-01 2.1581E-01 1.8672E-01 1.6262E-01 1.4239E-01 1.2526E-01 1.1180E-01 1.0096E-01 9.2034E-02 8.4558E-02
E(J)(MEV) = 7.8205E-02 7.2740E-02 6.7989E-02 6.3820E-02 6.0133E-02 5.6849E-02 5.3905E-02 5.1251E-02 4.8846E-02 4.6657E-02
E(J)(MEV) = 4.4655E-02
WAVE(J) = 7.7190E-01 8.2154E-01 8.8111E-01 9.5259E-01 1.0384E+00 1.1413E+00 1.2648E+00 1.4130E+00 1.5909E+00 1.8044E+00
WAVE(J) = 2.3678E+00 2.7367E+00 3.1424E+00 3.5897E+00 4.0796E+00 4.5703E+00 5.0614E+00 5.5523E+00 6.0432E+00
WAVE(J) = 6.5341E+00 7.0250E+00 7.5160E+00 8.0069E+00 8.4978E+00 8.9887E+00 9.4796E+00 9.9705E+00 1.0461E+01 1.0952E+01
WAVE(J) = 1.1443E+01
DWAVE(J) = 2.4880E-02 5.4604E-02 6.5525E-02 7.8630E-02 9.4355E-02 1.1323E-01 1.3587E-01 1.6305E-01 1.9566E-01 2.3479E-01
DWAVE(J) = 2.8174E-01 3.3809E-01 3.8727E-01 4.2600E-01 4.6840E-01 4.9091E-01 4.9091E-01 4.9091E-01 4.9091E-01 4.9091E-01
DWAVE(J) = 4.9091E-01 4.9091E-01 4.9091E-01 4.9091E-01 4.9091E-01 4.9091E-01 4.9091E-01 4.9091E-01 4.9091E-01 4.9091E-01
ANGULAR QUADRATURE AND WEIGHT
WP(IP) = 0.992400 0.911740 0.638520 0.219185 -0.219185 -0.638520 -0.911740 -0.992400
WP(IP) = 0.015190 0.146140 0.400300 0.438370 0.438370 0.400300 0.146140 0.015190
WPQ(IP) = 0.023860 0.023860 0.229557 0.251517 0.37275 0.37275 0.251517 0.023860 0.258222 0.172148 0.172148 0.258222
WPQ(IP) = 0.258222 0.258222 0.37275 0.37275 0.251517 0.229557 0.229557 0.023860 0.023860
PSY(P,PQ) = 0.785400 0.785400 0.314160 0.194350 2.356200 2.356200 1.099560 0.687225
PSY(P,PQ) = 0.0 0.0 2.042040 1.274300 0.0 0.0 2.827440 1.865330
PSY(P,PQ) = 0.0 0.0 0.0 2.654400 0.0 0.0 0.0 2.945300
PSYB(P,PQ) = 1.570800 1.570800 0.628320 0.392700 0.0 0.0 1.570800 0.981750
PSYB(P,PQ) = 0.0 0.0 2.513280 1.570800 0.0 0.0 0.0 2.159900
PSYB(P,PQ) = 0.0 0.0 0.0 2.748900
SPATIAL MESH ASSIGNMENT
RADIUS(CM) = 2.0000E+02 4.0000E+02 6.0000E+02 8.0000E+02 1.0000E+03 1.2000E+03 1.4000E+03 1.6000E+03 1.8000E+03 2.0000E+03
RADIUS(CM) = 2.0000E+03 2.0100E+03 2.0200E+03 2.0300E+03 2.0400E+03 2.0500E+03 2.0500E+03 2.0500E+03 2.0500E+03 2.0500E+03
RADIUS(CM) = 6.0500E+03 7.0500E+03 8.0500E+03 9.0500E+03 1.0050E+04 1.1050E+04 1.2050E+04 1.3050E+04 1.4050E+04 1.5050E+04
RADIUS(CM) = 2.4050E+04 2.8050E+04 3.2050E+04 3.6050E+04 4.0050E+04 4.4050E+04 4.8050E+04 5.2050E+04 5.6050E+04 6.0050E+04
RADIUS(CM) = 6.4050E+04 6.8050E+04 7.2050E+04 7.6050E+04 8.0050E+04 8.4050E+04 8.8050E+04 9.2050E+04 9.6050E+04 1.0005E+05
RADIUS(CM) = 1.0405E+05 1.0805E+05 1.1205E+05
Z-MESH(CM) = 0.0 8.0000E+00 1.6000E+01 2.4000E+01 3.2000E+01 4.0000E+01 4.8000E+01 5.6000E+01 6.4000E+01 7.2000E+01
Z-MESH(CM) = 1.0320E+03 1.5320E+03 2.0320E+03 2.5320E+03 3.0320E+03 3.5320E+03 4.0320E+03 4.5320E+03 5.0320E+03 5.5320E+03
Z-MESH(CM) = 1.5532E+04 1.8532E+04 2.1532E+04 2.4532E+04 2.7532E+04 3.0532E+04 3.3532E+04 3.6532E+04 3.9532E+04 4.2532E+04
Z-MESH(CM) = 4.5532E+04 4.8532E+04 5.1532E+04 5.4532E+04 5.7532E+04 6.0532E+04 6.3532E+04
LRR, LZ1, LZ2, LZR, LRMIN,LRMAX, IZR, IYR = 30 1 10 1 10
ROLD = 6.6660E+01 1.3333E+02 2.0000E+02 2.6666E+02 3.3333E+02 4.0000E+02 4.6666E+02 5.3333E+02 6.0000E+02 6.6666E+02
ROLD = 7.3333E+02 8.0000E+02 8.6666E+02 9.3333E+02 1.0000E+03 1.0667E+03 1.1333E+03 1.2000E+03 1.2667E+03 1.3333E+03
ROLD = 1.4000E+03 1.4667E+03 1.5333E+03 1.6000E+03 1.6667E+03 1.7333E+03 1.8000E+03 1.8667E+03 1.9333E+03 2.0000E+03
E = 6.620E-01

```

Fig.19-2 List of input data for Sample problem 4


```

.....*.....1.....*.....2.....*.....3.....*.....4.....*.....5.....*.....6.....*.....7.....*.....8
1  SAMPLE PROBLEM 5 PAL2DRZ.DATA(STREAM) 14 MEV NEUTRON BOUNDARY SOURCE 1
2  1 2 1 0 10 0 2
3  25 4 6-25 0 51 3
4  10 3 0 0 0 2 4
5  14.20 0.10 5
6  3 6 11 11 6
7  5.00 20.00 140.0 300.0 7
8  2 4 2 21 2 2 8
9  1.00 210.0 50.00 200.0 200.0 300.0 9
10 1 20 1 1 1 1 5 10
11 1.0 11
12 0 0 12
13 0.0 13
14 1 1 1 1 14
15 1 1 1 1 15
16 1 1 1 1 16
17 0 4 4 4 17
18 1 1 1 1 18
19 1 1 1 1 19
20 1 1 1 1 20
21 1 1 1 1 21
22 1 1 1 1 22
23 0 32 32 32 23
24 1 1 1 1 24
25 1 1 1 1 25
26 20 3 2 1 1 1 26
27 0 0 0 0 27
28 0 0 0 0 28
29 1 1 1 0 29
30 1 1 1 0 30
31 1 1 1 0 31
32 1 1 0 0 32
33 20 3 29 3 1 1 33
34 0 0 0 0 34
35 0 0 0 0 35
36 0 0 0 0 36
37 0 0 0 0 37
38 1 1 1 1 38
39 1 1 1 1 39
40 AIR 40
41 N 41
42 1074 5.000E-05 42
43 CONCRE 43
44 HY 44
45 1011 0.01213 45
46 OXY 46
47 1086 0.04725 47
48 SI 48
49 1140 0.01703 49
50 CA 50
.....*.....1.....*.....2.....*.....3.....*.....4.....*.....5.....*.....6.....*.....7.....*.....8

```

Fig.20-1 Input data for Sample problem 5

1.....*2.....*3.....*4.....*5.....*6.....*7.....*8			
51	1200	0.0045							51		
52	0	0							52		
53	0	0	0	0	0	1	6	14	33	53	
54	27	4	6-27	0	52					54	
55	10	3								55	
56	14.20		0.20							56	
57	3	6	11	11						57	
58	5.00		20.00		140.0		300.0			58	
59	2	4	2	21	2	2				59	
60	1.00		210.0		50.0		200.0		200.0	300.0	60
61	0	0									61
62	0.0										62
63	1	1	1	1							63
64	1	1	1	1							64
65	1	1	1	1							65
66	0	4	4	4							66
67	1	1	1	1							67
68	1	1	1	1							68
69	1	1	1	1							69
70	1	1	1	1							70
71	1	1	1	1							71
72	0	32	32	32							72
73	1	1	1	1							73
74	1	1	1	1							74
75	20	3	2	1	1	1					75
76	0	0	0	0							76
77	0	0	0	0							77
78	0	0	0	0							78
79	0	0	0	0							79
80	0	0	0	0							80
81	0	0	0	0							81
82	20	3	29	3	1	1					82
83	0	0	0	0							83
84	0	0	0	0							84
85	0	0	0	0							85
86	0	0	0	0							86
87	1	1	1	1							87
88	1	1	1	1							88
89	AIR										89
90	N										90
91	2074	5.000E-05									91
92	CONCRE										92
93	HY										93
94	2011	0.01213									94
95	OXY										95
96	2086	0.04725									96
97	SI										97
98	2140	0.01703									98
99	CA										99
100	2200	0.0045									100

Fig.20-2 (Continued)

	1	2	3	4	5	6	7	8			
101	0	0							101		
102	0	0	0	0	0	1	6	14	33	102	
103	45	4	6-45	0	54					103	
104	10	3								104	
105	14.20		0.40							105	
106	3	6	11	11						106	
107	5.00		20.00		140.0		300.0			107	
108	2	4	2	21	2	2				108	
109	1.00		210.0		50.00		200.0		200.0	300.0	109
110	10	90									110
111	0.01										111
112	1	1	1	1							112
113	1	1	1	1							113
114	1	1	1	1							114
115	0	4	4	4							115
116	1	1	1	1							116
117	1	1	1	1							117
118	1	1	1	1							118
119	1	1	1	1							119
120	1	1	1	1							120
121	0	32	32	32							121
122	1	1	1	1							122
123	1	1	1	1							123
124	20	3	2	1	1	1					124
125	0	0	0	0							125
126	0	0	0	0							126
127	0	0	0	0							127
128	0	0	0	0							128
129	0	0	0	0							129
130	0	0	0	0							130
131	20	3	29	3	1	1					131
132	0	0	0	0							132
133	0	0	0	0							133
134	0	0	0	0							134
135	0	0	0	0							135
136	1	1	1	1							136
137	1	1	1	1							137
138	AIR										138
139	N										139
140	4074	5.000E-05									140
141	CONCRE										141
142	HY										142
143	4011	0.01213									143
144	OXY										144
145	4086	0.04725									145
146	SI										146
147	4140	0.01703									147
148	CA										148
149	4200	0.0045									149
150	0	0									150
151	0	0	0	0	0	1	6	14	33		151

*** INPUT DATA END ***

Fig.20-3 (Continued)

```

*** INPUT DATA
SAMPLE PROBLEM 5 PAL2DRZ.DATA(STREAM) 14 MEV NEUTRON BOUNDARY SOURCE *****
KNDG,KIN,NORF,KTST,MONDE,MNODRE,IPRNT,IRZR,IRIZ = 1 2 1 0 10 0 0 0 0 0

INPUT DATA NO.1

E-MAX = 1.420E+01 ENERGY MESH = 25 LETHARGY WIDTH= 1.000E-01
SOURCE NORMALIZATION = 0.0 NNI( LIB-DISK NO.) = 51

UNCOLLIDED FLUX CAL. OPTION = -1 FISSION SOURCE = 0 START ENERGY MESH = 1

REGION 1 2 3 4 5 6 7 8 9 10
R-MESHES = 3 6 11
R-THICKNESS = 5.000E+00 2.000E+01 1.400E+02 3.000E+02
Z-MESHES = 2 4 2 21
Z-THICKNESS = 1.000E+00 2.100E+02 5.000E+01 2.000E+02 2.000E+02 3.000E+02

NBND,IB1,IB2Z,IBR,LTAP,JOAK,IRWTR = 10 3 0 0 0 2 0

ENERGY POINTS(MEV)
E(J)(MEV) = 1.4200E+01 1.2849E+01 1.1626E+01 1.0520E+01 9.5185E+00 8.6127E+00 7.7931E+00 7.0515E+00 6.3805E+00 5.7733E+00
E(J)(MEV) = 5.2239E+00 4.7268E+00 4.2779E+00 3.8700E+00 3.5017E+00 3.1684E+00 2.8669E+00 2.5941E+00 2.3472E+00 2.1239E+00
E(J)(MEV) = 1.9218E+00 1.7389E+00 1.5734E+00 1.4237E+00 1.2882E+00

ANGULAR QUADRATURE AND WEIGHT
WP(IP) = 0.992400 0.911740 0.638320 0.219185 -0.219185 -0.638320 -0.911740 -0.992400
WPP(IP) = 0.015190 0.146140 0.400300 0.438370 0.438370 0.400300 0.146140 0.015190
WPA(IP) = 0.023860 0.023860 0.229557 0.229557 0.251517 0.377275 0.377275 0.251517 0.258222 0.258222
WPA(IP) = 0.258222 0.258222 0.172148 0.172148 0.258222 0.258222 0.258222 0.258222 0.258222 0.172148
WPA(IP) = 0.251517 0.377275 0.377275 0.229557 0.229557 0.229557 0.229557 0.229557 0.229557 0.229557
PSY(P,PQ) = 0.785400 0.785400 0.314160 0.196350 0.314160 0.314160 0.196350 0.314160 0.785400 0.785400
PSY(P,PQ) = 0.0 0.0 2.042040 1.276300 0.0 0.0 2.827440 1.865330 2.945300 1.570800
PSYB(P,PQ) = 1.570800 1.570800 0.628320 0.392700 0.0 0.0 1.570800 0.981750
PSYB(P,PQ) = 0.0 0.0 2.513280 1.570800 0.0 0.0 0.0 0.0 2.159900
PSYB(P,PQ) = 0.0 0.0 0.0 2.748900

SPATIAL MESH ASSIGNMENT
RADIUS(CM) = 1.667E+00 3.333E+00 5.000E+00 5.000E+00 9.000E+00 1.3000E+01 1.7000E+01 2.1000E+01 2.5000E+01 2.5000E+01
RADIUS(CM) = 3.9000E+01 5.3000E+01 6.7000E+01 8.1000E+01 9.5000E+01 1.0900E+02 1.2300E+02 1.3700E+02 1.5100E+02 1.6500E+02
RADIUS(CM) = 1.6500E+02 1.9500E+02 2.2500E+02 2.5500E+02 2.8500E+02 3.1500E+02 3.4500E+02 3.7500E+02 4.0500E+02 4.3500E+02
RADIUS(CM) = 4.6500E+02
Z-MESH(CM) = 0.0
Z-MESH(CM) = 2.8100E+02 2.9100E+02 3.0100E+02 3.1100E+02 3.2100E+02 3.3100E+02 3.4100E+02 3.5100E+02 3.6100E+02 3.7100E+02
Z-MESH(CM) = 3.8100E+02 4.0100E+02 4.2100E+02 4.4100E+02 4.6100E+02 4.8100E+02 5.0100E+02 5.2100E+02 5.4100E+02 5.6100E+02
Z-MESH(CM) = 5.8100E+02 6.0100E+02 6.2100E+02 6.4100E+02 6.6100E+02 6.8100E+02 7.0100E+02 7.2100E+02 7.4100E+02 7.6100E+02

LRMIN,LRMAX, ISOTROPIC ANG.DIS.,CONST SOURCE DIS. IRPT,IXR, IYR = 1 20 1 1 1 1 5
SE(N) = 1.0000E+00

BOUNDARY CONDITION
ENERGY MESH = 1
BOUND = 1.5915E-01 1.5915E-01 1.5915E-01 1.5915E-01 1.5915E-01 1.5915E-01 1.5915E-01 1.5915E-01 1.5915E-01 1.5915E-01
BOUND = 1.5915E-01 1.5915E-01 1.5915E-01 1.5915E-01 1.5915E-01 1.5915E-01 1.5915E-01 1.5915E-01 1.5915E-01 1.5915E-01
BOUND = 1.5915E-01 1.5915E-01 1.5915E-01 1.5915E-01 1.5915E-01 1.5915E-01 1.5915E-01 1.5915E-01 1.5915E-01 1.5915E-01
BOUND = 1.5915E-01 1.5915E-01 1.5915E-01 1.5915E-01 1.5915E-01 1.5915E-01 1.5915E-01 1.5915E-01 1.5915E-01 1.5915E-01
BOUND = 1.5915E-01 1.5915E-01 1.5915E-01 1.5915E-01 1.5915E-01 1.5915E-01 1.5915E-01 1.5915E-01 1.5915E-01 1.5915E-01
BOUND = 1.5915E-01 1.5915E-01 1.5915E-01 1.5915E-01 1.5915E-01 1.5915E-01 1.5915E-01 1.5915E-01 1.5915E-01 1.5915E-01
BOUND = 1.5915E-01 1.5915E-01 1.5915E-01 1.5915E-01 1.5915E-01 1.5915E-01 1.5915E-01 1.5915E-01 1.5915E-01 1.5915E-01
BOUND = 1.5915E-01 1.5915E-01 1.5915E-01 1.5915E-01 1.5915E-01 1.5915E-01 1.5915E-01 1.5915E-01 1.5915E-01 1.5915E-01

```

Fig.20-4 List of input data for Sample Problem 5

BOUN = 1.5915E-01 1.5915E-01 1.5915E-01 1.5915E-01 1.5915E-01
 ENERGY MESH = 2
 BOUN = 0.0 0.0 0.0 0.0 0.0 0.0 0.0 0.0 0.0 0.0
 BOUN = 0.0 0.0 0.0 0.0 0.0 0.0 0.0 0.0 0.0 0.0
 BOUN = 0.0 0.0 0.0 0.0 0.0 0.0 0.0 0.0 0.0 0.0
 BOUN = 0.0 0.0 0.0 0.0 0.0 0.0 0.0 0.0 0.0 0.0
 BOUN = 0.0 0.0 0.0 0.0 0.0 0.0 0.0 0.0 0.0 0.0
 BOUN = 0.0 0.0 0.0 0.0 0.0 0.0 0.0 0.0 0.0 0.0
 BOUN = 0.0 0.0 0.0 0.0 0.0 0.0 0.0 0.0 0.0 0.0
 BOUN = 0.0 0.0 0.0 0.0 0.0 0.0 0.0 0.0 0.0 0.0

LTHAL,LCUT,EPSRN = 0 0 0.0

NUMBER OF ELEMENT IN EACH REGION

NOEL = 1 1 1 1
 NOEL = 1 1 1 1
 NOEL = 1 1 1 1
 NOEL = 0 4 4 4
 NOEL = 1 1 1 1
 NOEL = 1 1 1 1

MATERIAL NUMBER OF EACH REGION

NEK = 1 1 1 1
 NEK = 1 1 1 1
 NEK = 1 1 1 1
 NEK = 0 32 32 32
 NEK = 1 1 1 1
 NEK = 1 1 1 1

INDICATOR OF SOURCE POSITION IN UNCLFX

KSRI,KBR1,KZT1,KBZ1,KZB1,KBBZ1,NPHI = 20 3 2 1 1 1 1 4

INDICATOR OF UNCL. CAL. UNCOLLIDED FLUXES

IUNC= 0 0 0 0
 IUNC= 0 0 0 0
 IUNC= 1 1 1 0
 IUNC= 1 1 1 0
 IUNC= 1 1 1 0
 IUNC= 1 1 0 0
 KSR2, KBR2, KZT2, KBZ2, KZB2, KBBZ2 = 20 3 29 3 1 1
 IUNB = 0 0 0 0
 IUNB = 0 0 0 0
 IUNB = 0 0 0 0
 IUNB = 0 0 0 0
 IUNB = 1 1 1 1
 IUNB = 1 1 1 1

TOTAL R-MESH = 31 TOTAL Z-MESH = 33
 JSAT,J11,J12,JJ,NNI(READ(NNI) DATA) = 1 1 25 25 51

**** NUCLEAR DATA ** Fig.20-5 (Continued)